CRCLEME
Cooperative Research Centre for
Landscape Evolution & Mineral Exploration

AMIRA
Australian Mineral Industries Research Association Limited ACN 004 448 266

OPEN FILE
REPORT
SERIES

REGOLITH LANDFORM RELATIONSHIPS AND GEOCHEMICAL DISPERSION AROUND TRINGADEE AND BRUMBY PROSPECTS, NORTH QUEENSLAND

C. Phang, T.J. Munday and J.E. Wildman

CRC LEME OPEN FILE REPORT 140

April 2002

(CSIRO Exploration and Mining Report 429R / CRC LEME Report 59R, 1997.
2nd Impression 2002.)

AMIRA
Australian Mineral Industries Research Association Limited ACN 004 448 266

CRCLEME
Cooperative Research Centre for
Landscape Evolution & Mineral Exploration

REGOLITH LANDFORM RELATIONSHIPS AND GEOCHEMICAL DISPERSION AROUND TRINGADEE AND BRUMBY PROSPECTS, NORTH QUEENSLAND

C. Phang, T.J. Munday and J.E. Wildman

CRC LEME OPEN FILE REPORT 140

April 2002

(CSIRO Exploration and Mining Report 429R / CRC LEME Report 59R, 1997.
2nd Impression 2002.)

CRC LEME is an unincorporated joint venture between CSIRO-Exploration & Mining, and Land & Water, The Australian National University, Curtin University of Technology, University of Adelaide, University of Canberra, Geoscience Australia, Bureau of Rural Sciences, Primary Industries and Resources SA, NSW Department of Mineral Resources-Geological Survey and Minerals Council of Australia.
Headquarters: CRC LEME c/o CSIRO Exploration and Mining, PO Box 1130, Bentley WA 6102, Australia

CSIRO/CRC LEME/AMIRA PROJECT P417
GEOCHEMICAL EXPLORATION IN REGOLITH-DOMINATED TERRAIN, NORTH QUEENSLAND 1994-1997

In 1994, CSIRO commenced a multi-client research project in regolith geology and geochemistry in North Queensland, supported by 11 mining companies, through the Australian Mineral Industries Research Association Limited (AMIRA). This research project, "Geochemical Exploration in Regolith-Dominated Terrain, North Queensland" had the aim of substantially improving geochemical methods of exploring for base metals and gold deposits under cover or obscured by deep weathering in selected areas within (a) the Mt Isa region and (b) the Charters Towers - North Drummond Basin region.

In July 1995, this project was incorporated into the research programs of CRC LEME, which provided an expanded staffing, not only from CSIRO but also from the Australian Geological Survey Organisation, University of Queensland and the Queensland Department of Minerals and Energy. The project, operated from nodes in Perth, Brisbane, Canberra and Sydney, was led by Dr R.R. Anand. It was commenced on 1st April 1994 and concluded in December 1997. The project involved regional mapping (three areas), district scale mapping (seven areas), local scale mapping (six areas), geochemical dispersion studies (fifteen sites) and geochronological studies (eleven sites). It carried the experience gained from the Yilgarn (see CRC LEME Open File Reports 1-75 and 86-112) across the continent and expanded upon it.

Although the confidentiality period of Project P417 expired in mid 2000, the reports have not been released previously. CRC LEME acknowledges the Australian Mineral Industries Research Association and CSIRO Division of Exploration and Mining for authority to publish these reports. It is intended that publication of the reports will be a substantial additional factor in transferring technology to aid the Australian mineral industry.

This report (CRC LEME Open File Report 140) is a second impression (second printing) of CSIRO, Division of Exploration and Mining Restricted Report 429R, first issued in 1997, which formed part of the CSIRO/AMIRA Project P417.

Copies of this publication can be obtained from:
The Publication Officer, c/- CRC LEME, CSIRO Exploration and Mining, P.O. Box 1130, Bentley, WA 6102, Australia.. Information on other publications in this series may be obtained from the above or from http://leme.anu.edu.au/

Cataloguing-in-Publication:
Phang, C.
Regolith landform relationships and geochemical dispersion around Tringadee and Brumby prospects, North Queensland.
ISBN 0 643 06822 8
1. Regolith - North Queensland 2. Landforms - North Queensland 3. Geochemistry
I. Munday, T.J. II. Wildman, J.E. III. Title
CRC LEME Open File Report 140.
ISSN 1329-4768

PREFACE AND EXECUTIVE SUMMARY

The CRC LEME-AMIRA Project 'Geochemical exploration in regolith-dominated terrain of North Queensland' (P417) has an overall aim of substantially improving geochemical methods of exploring for base metals and gold deposits under cover or obscured by deep weathering. The research includes geochemical dispersion studies, regolith characterisation, dating of profiles and investigation of regolith evolution.

This report addresses both regolith characterisation and dispersion of Zn at the Tringadee Prospect and Cu-Au at the Brumby Prospect, which are largely overlain by Mesozoic sediments. An area of 550 km^2 was mapped to provide a regolith-landform framework. Regionally, the area consists of low hills and mesas of Mesozoic sediments, hills and mesas developed on Proterozoic basement and alluvial plains with black, swelling, clay-rich soils.

Zinc has been laterally dispersed over some distance into the Mesozoic at the Tringadee Prospect and is associated with concentrations of Fe and Mn oxides, probably related to previous redox fronts. At the Brumby Prospect, horizontal ferruginous bands reflect the underlying mineralisation. In contrast, subvertical ferruginous veins give little indication of mineralisation, thus horizontal ferruginous bands should be sampled preferentially.

R. R. Anand

Project Leader

I.D.M. Robertson

Deputy Project Leader

CONTENTS

ABSTRACT

The purpose of this study is to investigate the origin of a Zn anomaly (up to 1000 ppm) in Mesozoic cover at Tringadee prospect. In the Brumby prospect, ferruginous materials developed in Mesozoic cover at the surface or subsurface were studied to find any indication of concealed mineralisation. District scale regolith mapping of approximately 550 km^2 was carried out to provide a framework for a geochemical dispersion study of the two prospects. Stratigraphic relationships of the main regolith units were also established to provide constraints for the interpretation of the regolith geochemistry.

Three major geomorphic environments can be delineated in Tringadee area. These are i) the low hills and mesas developed in Mesozoic sediments in the central zone ii) the low hills and mesas developed on the Proterozoic basement in the north and west and iii) the depositional plains with brown and well-developed 'black' clay soils over recent alluvial materials to the south and south-east. Contrasting lithologies combined with erosion, deposition, ferruginisation and silicification are important factors contributing to the variation in regolith materials and landforms observed in the area.

At the Tringadee Prospect, the Zn anomaly in the Mesozoic sediments appears to be associated with accumulated Fe and Mn oxides. The area is interpreted to have remained in a low part of the landscape before, during and after deposition of the Mesozoic sediments. Iron, Mn and Zn appear to have derived from external sources and have migrated laterally along permeable layers, precipitating at redox fronts within the sediment pile. This probably occurred after deposition, but contemporaneous accumulation of the metals with the sediments is possible. It is considered that the source of the Zn is external and that it has been scavenged by Fe-Mn oxide precipitates, now represented by ferruginous bands. There is thus no relationship between Zn anomalies in the sedimentary cover and potential base metal mineralisation in the basement.

The Brumby prospect has subvertical ferruginous veins in the Mesozoic, probably associated with faulting of the underlying Proterozoic and appear to form remnants of conduits for fluids rich in Fe. The ferruginous veins give no indication of mineralisation. In contrast, the subhorizontal ferruginous bands associated with redox zones or permeability layers within the sediment pile are preferentially sampled.

1. INTRODUCTION

The Tringadee area lies within the Eastern Succession, 120 km south of Cloncurry and west of Cannington Station (Figure 1). The area is of generally low relief, largely comprising extensive depositional plains covered by well-developed black clay soils over recent alluvium. The black soils are common to the south and southeast and are generally 1-2 m thick. The plains are interspersed with isolated low hills and mesas that rise generally <30 m above a mean altitude of 300 m amsl. Low hills and mesas of Mesozoic sediments dominate the central portion of the area. Similar landforms developed on the Proterozoic basement characterise the north and westerly portions of the mapped area.

District-scale regolith-landform mapping of approximately 550 km^2 has resulted in a 1:50,000 scale regolith-landform map which forms the framework for a geochemical dispersion study of the Tringadee Zn and Brumby Cu-Au prospects, identified by Aberfoyle Resources Ltd by drilling magnetic anomalies through the Mesozoic sedimentary cover. Stratigraphic relationships of the main regolith units were also defined to constrain the interpretation of the regolith geochemistry.

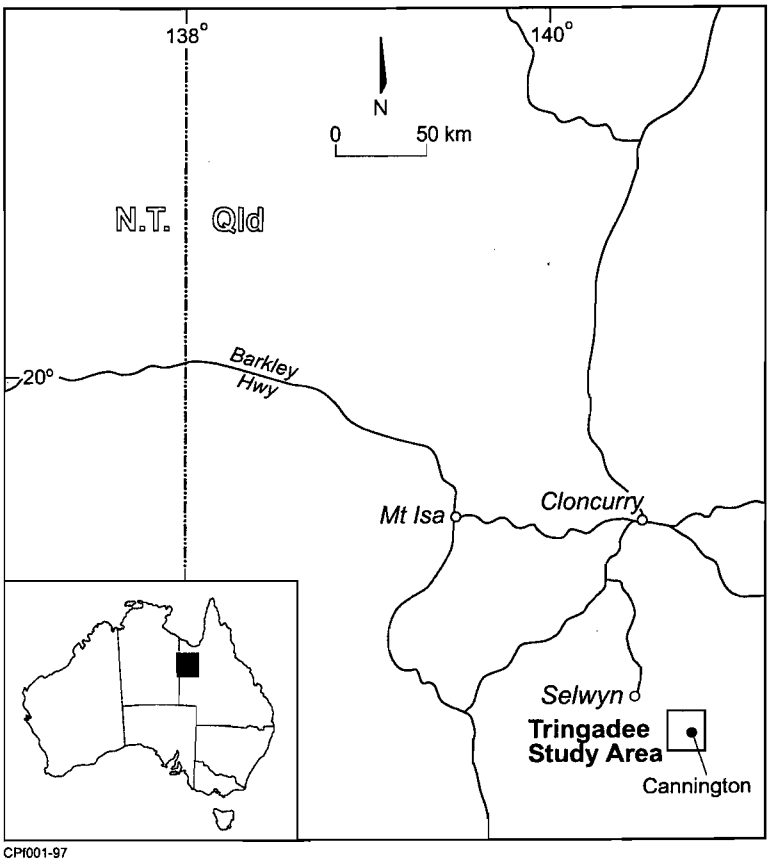

Figure 1. Location map of study area

The Tringadee Prospect features a Zn anomaly (up to 1000 ppm) in Mesozoic cover (Aberfoyle Resources Ltd unpublished data). Two RAB drill intersections ROTR 155 (at 479500 mE 7580000 mN) and ROTR 156 (at 479500 mE 7580000 mN) with Zn anomalies >1000 ppm were examined to investigate their origin. The Brumby (Cu-Au) prospect (at 475240 mE 7584595 mN) is situated in low hills of Mesozoic sediments. Surficial ferruginous veins and subsurface ferruginous bands developed in the sediments were used to determine whether they indicate concealed mineralisation in the Proterozoic basement. Partial extractions were also undertaken to increase the contrast of gold or copper response.

2. REGIONAL SETTING AND LOCAL GEOLOGY

The Tringadee area sits on the southeastern portion of the Selwyn Region which has a semi-desert tropical climate, with annual rainfall averaging 375 mm. The vegetation consists mainly of spinifex and sparse low trees and shrubs. Pockets of dense to open scrub of 'turpentine' bush (*Acacia lysiphloia*) are common, with eucalypts growing along main watercourses.

Variably eroded Mesozoic sediments lying on the margin of the Eromanga Basin characterise the Tringadee area. This thins to the north of the study area, where Proterozoic porphyritic biotite granite outcrops. The Mesozoic sediments comprise siltstones with a basal sandstone and conglomerate. A simplified version of the local geology of the area is shown in Figure 2. All the drainages through the Tringadee area run southwards, the main drainage being Bustard Creek which drains into the Hamilton River.

3. REGOLITH DISTRIBUTION, STRATIGRAPHIC RELATIONSHIPS AND CHARACTERISTICS

3.1 Regolith-landform mapping

A framework of regolith distribution and stratigraphy was established for the district surrounding the Tringadee Zn and Brumby Cu-Au prospects as a basis for geochemical dispersion studies. A regolith-landform map at 1:50 000 scale (Appendix I), which covers approximately 550 km^2, was produced from a combined interpretation of colour air photographs (1:25 000 scale), enhanced Landsat TM imagery (Figure 3), published geological maps (1:100 000 map sheet 7054, Selwyn) and field traverses and study of RAB intersections.

Important factors contributing to the variation in regolith materials and landforms observed in this area are the contrasting lithologies combined with processes of erosion, deposition, ferruginisation and silicification. Three major geomorphic environments can be delineated. These are i) the low hills and mesas developed in Mesozoic sediments in the central zone (Figure 4A), ii) the low hills and mesas developed on the Proterozoic basement in the north and west (Figure 4B) and iii) the depositional plains with brown and well-developed 'black' clay soils over alluvium to the south and southeast (Figure 4C).

3.2 Low hills and mesas developed on Mesozoic sediments

A schematic presentation of dominant regolith-landform regimes in this environment is shown in Figure 5. A variety of regolith materials occur in the area. The remnant Mesozoic sediments stand out as mesas, with local relief of <30 m. They tend to have patchy remnant lateritic cappings at their top. Some mesas have been eroded to isolated low, conical hills or buttes. The Mesozoic sediments in the Tringadee area are mainly siltstone with poorly sorted and commonly cross-bedded, sandy to conglomeratic rocks at the base. Much of the upper part of the Mesozoic sediments has been silicified to porcellanite, commonly brecciated and cut across by conchoidal fractures that have

formed the loci for Fe acccumulation. On Landsat TM imagery (Figure 3), silicification and ferruginisation show as yellow hues.

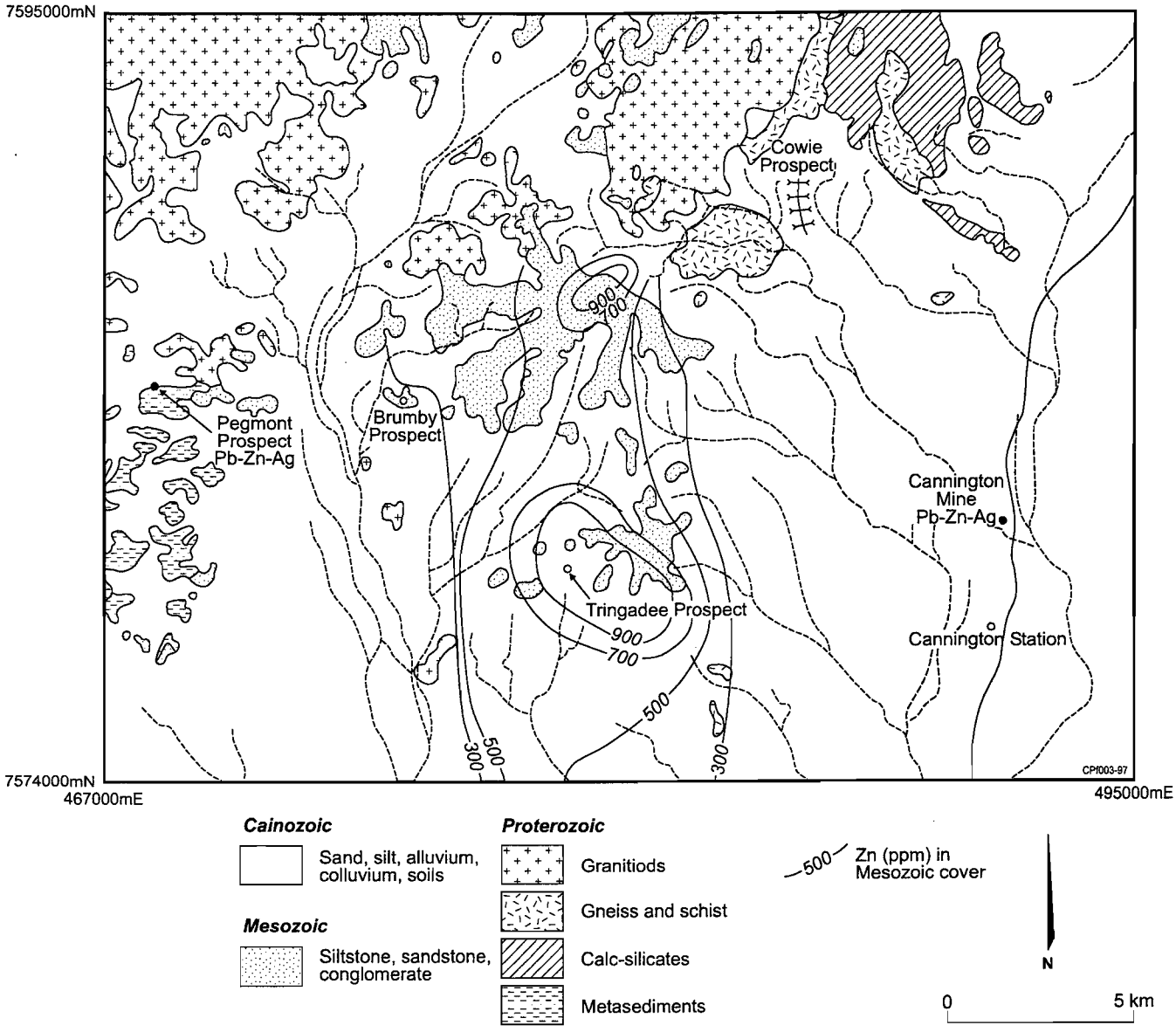

Figure 2. Simplified geological map of the Tringadee Prospect (Zn anomaly contours from Aberfoyle Resources Ltd).

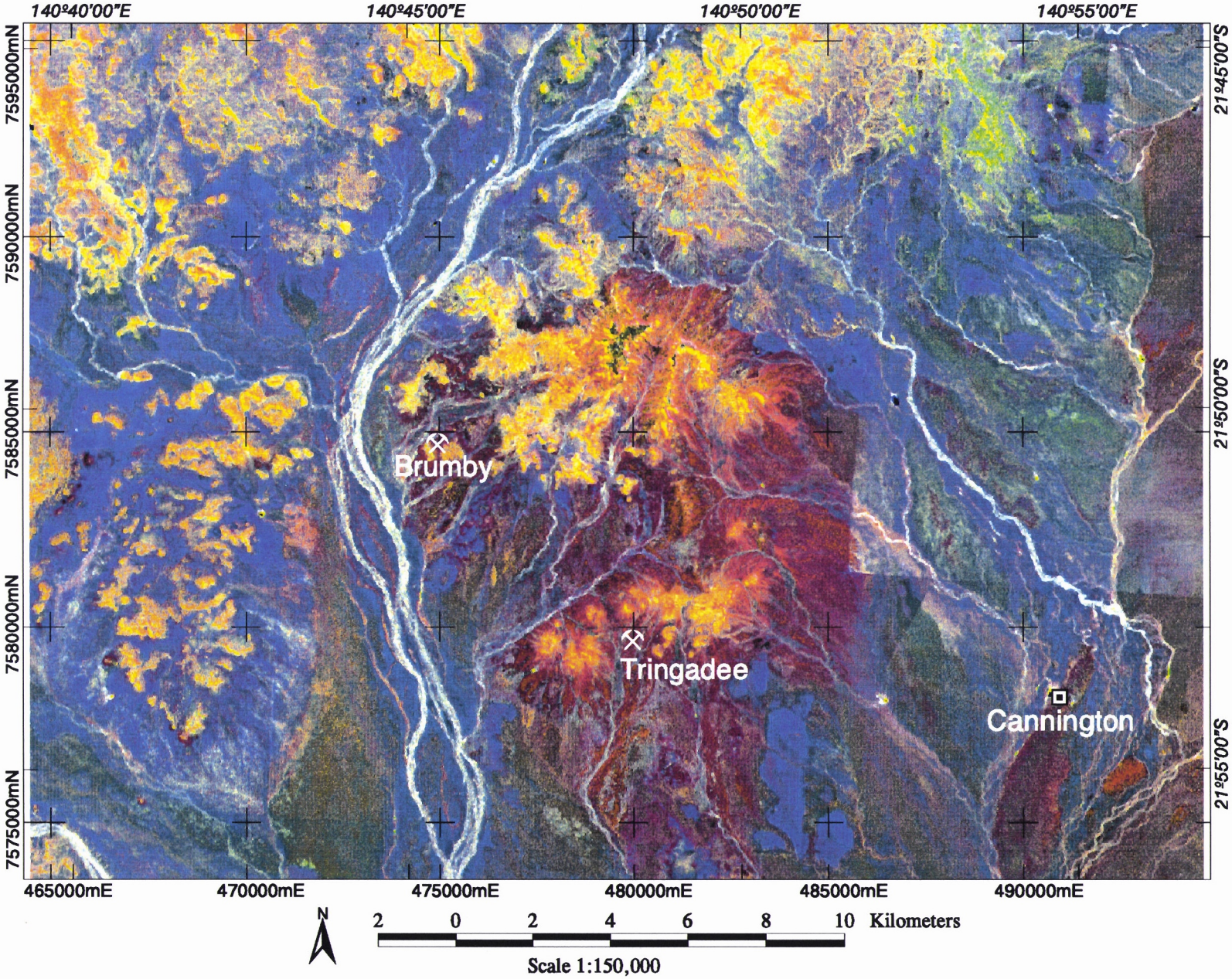

Figure 3: Landsat TM ratio colour composite of the Tringadee area (TM band ratios 5/7 (red), 4/7 (green) and 4/2 (blue). Yellows are indicative of silicification and ferruginisation which characterise Proterozoic and Mesozoic rocks. Blues are indicative of sandy colluvial/alluvial outwash plains. Red-purple hues relate to polymict lag dominated by ferruginised lithic fragments.

FIGURE 4

THREE MAJOR GEOMORPHIC ENVIRONMENTS

A. Low hills and mesas developed on Mesozoic sediments. On top of these hills and mesas are brown, brecciated Fe-stained and mottled silicified saprolite (1) which are underlain by pale silicified saprolite (2). The view is west from AMG 479000 mE, 7585600 mN, Zone 54K.

B. Low hills and mesas developed on Proterozoic granites. The granites are deeply weathered into mottled saprolite (1) with evidence of silicification in the upper part of the profile. In places, a remnant veneer of Mesozoic sediments (2) is found on the mesas. The view is towards the north from AMG 469450 mE, 7588970 mN, Zone 54K.

C. Depositional plains which comprise extensive black soils (1) and polymictic ferruginous lag (2). A boulder of brecciated Fe-stained and mottled silicified saprolite is shown in (3). The view is east from AMG 483000 mE, 7581140 mN, Zone 54K.

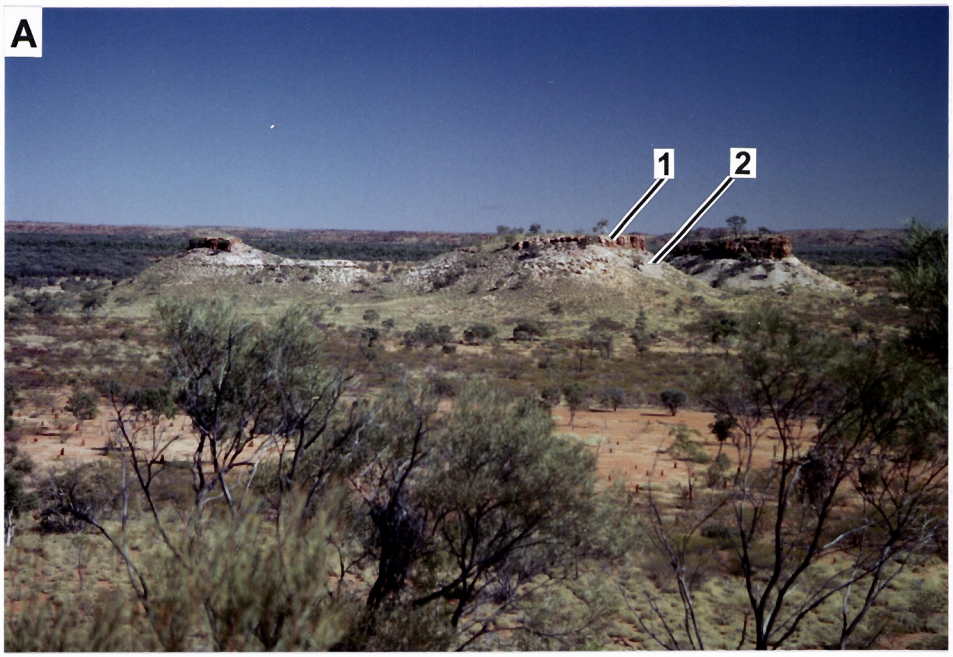
A
1
2

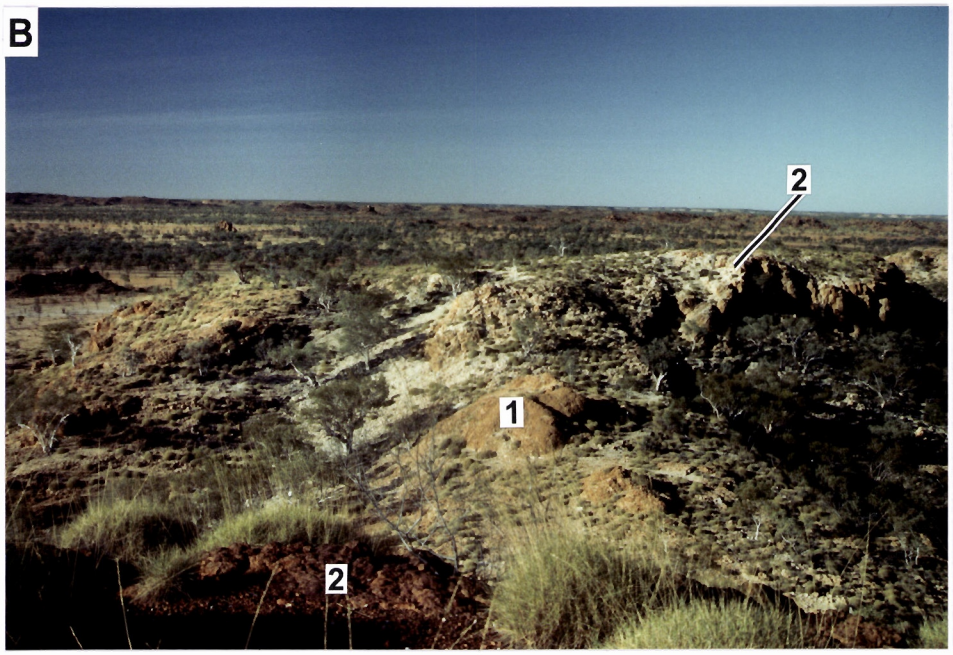
B
2
1
2

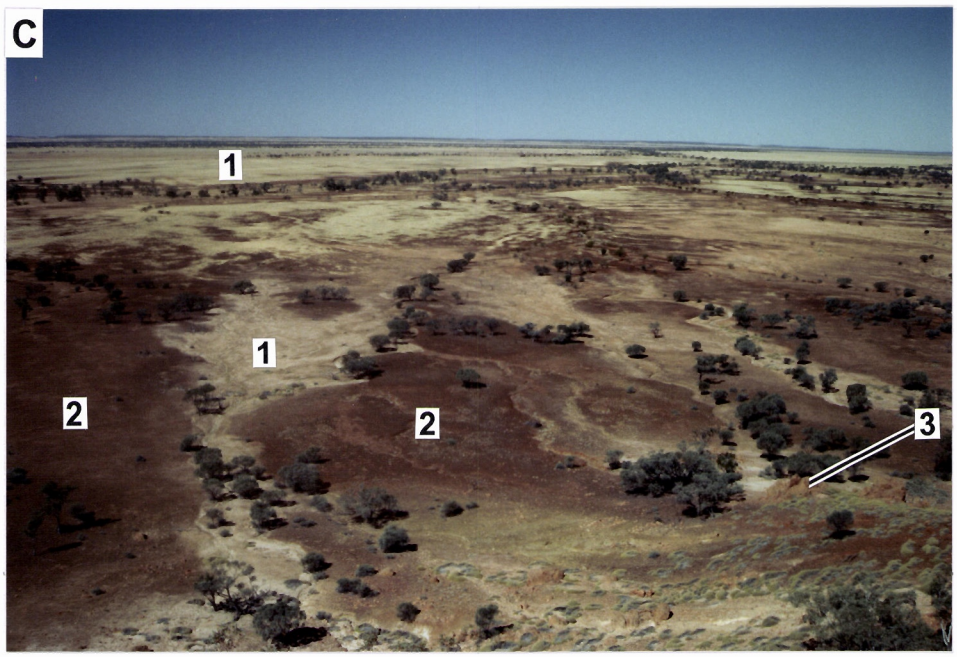
C
1
1
2
2
3

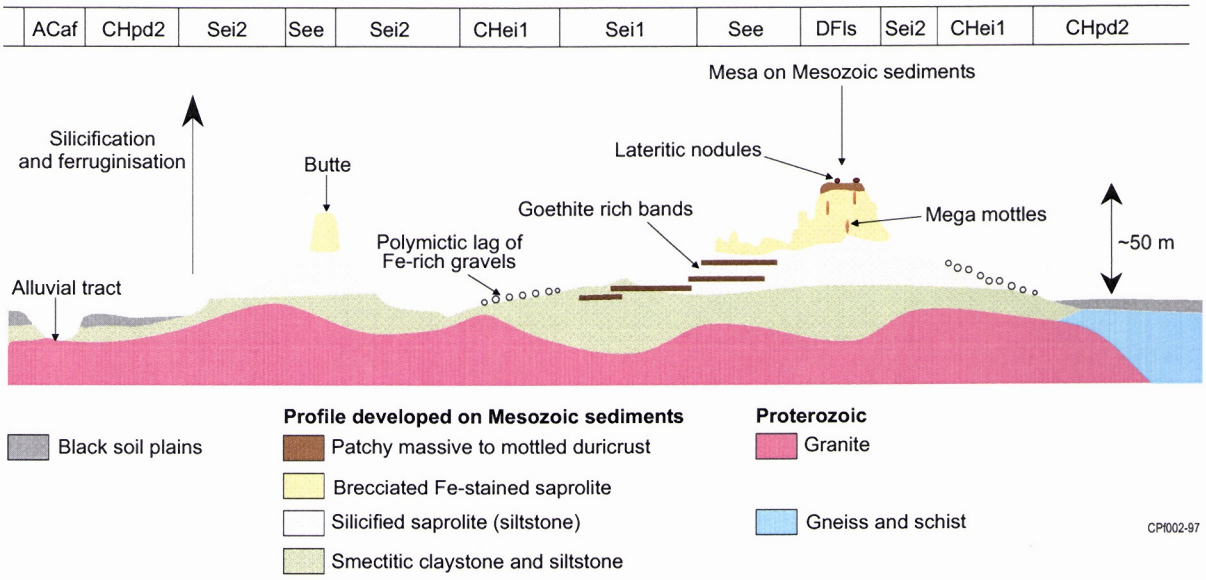

Figure 5. Regolith-landform units developed in Mesozoic sediments.

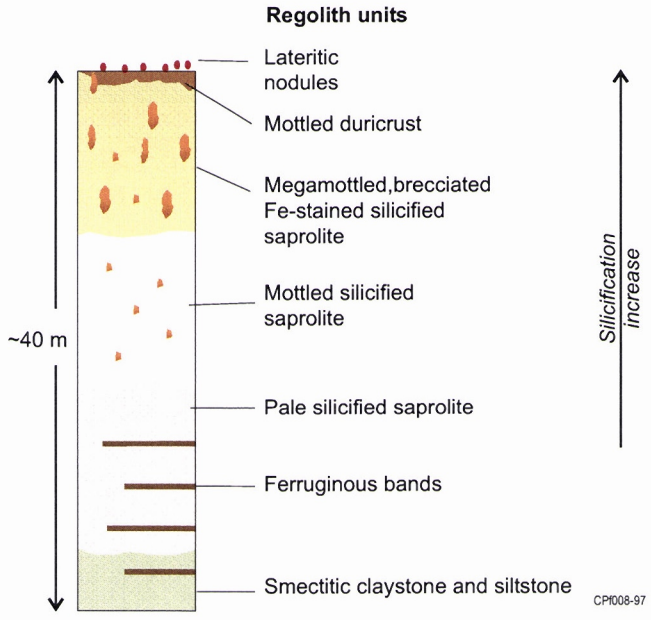

Figure 6. Schematic vertical section of weathering profile in Mesozoic sediments.

A typical weathering profile over Mesozoic siltstone is shown schematically in Figure 6. Pockets of remnant lateritic capping with a lag of lateritic nodules and patchy, mottled duricrust are confined to the top of mesas and buttes (map unit DFls; Figure 7A). The lateritic nodules (TG 72,74 in Table A1-Appendix III; Figure 8A) are generated by physical breakdown of mottled duricrust or, in places, mega mottles. The mottled duricrust (TG73 in Table A1-Appendix III; Figure 8B) contains mainly goethite, with some hematite, and is concentrated as coatings in voids and as infillings of fractures in the siltstone, forming a network. Silica occurs mainly as quartz, with some opal-CT. The mottled duricrust and the nodules are rich in V (2500-9000 ppm) and are enriched in Si, Al, Pb, Ba and Cr compared to other regolith units on the mesa. The collapse of the saprolite, through removal of the clay matrix by leaching, induces brecciation and fragmentation. This destabilises the weathering profile and causes slumping and mass wasting of the overlying regolith. Elliptical weathering hollows, with annular ridges of about 1 m diameter, occur near the tops of the mesas and are filled with ferruginous nodules. Within the siltstone, fine sandy layers occur. Percolation of Fe-rich fluids through these porous, sandy layers form ferruginous bands, which are more common lower in the profile.

Escarpments are typical in areas occupied by brecciated, Fe-stained and mottled silicified saprolite, which forms a siliceous breccia in a yellowish brown clay matrix (map unit See; TG502 in Table A1-Appendix III; Figures 7B and 8C). In places, the brecciated Fe-stained saprolite stands out as steep, faceted turrets. Blocky megamottles occur sporadically in this brecciated zone (Figure 7D). The saprolite matrix is a highly siliceous porcellanite, of quartz and opal-CT (TG75 in Table A1-Appendix III).

The pediments flanking the Mesozoic mesas and low hills contain deeply incised gullies with highly erodible pale to greyish brown, saprolitic clays (map unit Sei2; Figure 7C). These clays are smectitic and contain some kaolinite, goethite and mica (TG79,128F-130F in Table A1-Appendix III). The pediments, in places, expose ferruginous, subhorizontal bands in step-like microrelief (map unit Seil). In certain sites, these ferruginous bands are reworked to low knolls which are goethite and Mn rich and characteristically ochre stain the surrounding saprolite. They also contain quartz, some mica and kaolinite (TG 147 in Table A1-Appendix III; Figure 8E). A widespread veneer of polymictic lag of Fe-rich gravels, quartz gravels and silicified and brecciated siltstone fragments (map unit CHeil; Figure 7E), caused by colluvial outwash, covers a major portion of the pediments, reflected in the Landsat imagery (Figure 3) as dark- red hues.

3.3 Low hills and mesas developed on the Proterozoic basement

A schematic transect representing main regolith-landforms of the Proterozoic basement is shown in Figure 9. The Proterozoic bedrock consists mainly of granitoids with pockets of calc-silicate and amphibolites in the north and some metasediments towards the west. The landforms in this area are similar to the Mesozoic environment; low hills are more characteristic of the Proterozoic. The alluvium-colluvium is red due to dominant red Fe-stained quartzitic sands derived from the granitoids.

A schematic vertical section of a typical weathering profile over granite is given in Figure 10. Pockets of lateritic nodules with patchy ferruginous duricrust (map unit Dfel; TG204 and TG205 in Table A1-Appendix III) are limited to the tops of mesas. The ferruginous duricrust consists of pisoliths (Figure 8D) cemented with ferruginous saprolite fragments of the Proterozoic granite. There is evidence of silicification in the upper part of the weathering profile. In places, the mesas support a remnant lateritic profile of the Mesozoic sediments above. The unconformity between the Mesozoic and Proterozoic is commonly characterised by a coarser sand and conglomerate which is generally ferruginised. (Figure 7J).

Towards the north part of the central area, a ferruginous vein (Figure 7I) related to late-stage hydrothermal activity associated with granite emplacement, cuts across the granitiod terrain. This vein now consists dominantly of hematite with some goethite, kaolinite and mica and has a microscopic trellis fabric (martite) that indicates derivation from magnetite (TG189 in Table A1-Appendix III; Figure 8H). The hematite is rich in Mn and Co compared to other regolith materials. The trellis microfabric is also common in lateritic nodules over granite, indicating a likelihood that the weathering of these magnetite veins has contributed to the lag of lateritic nodules. In areas of low hills and erosional rises, the regolith consists of mottled saprolite with minor outcropping granitic saprock (map unit Sel1). The weathered granite contains white patches of kaolinite from the weathering of feldspars and reddish hematitic mottles from weathered biotite (TG 511 in Table 1A-Appendix III).

Sheetflow deposits, consisting of red, colluvial-alluvial sands and sporadic, subangular quartz pebbles, derived from breakdown of quartz veins, occur around the apron of the low hills (map unit CHei2; Figure 7K). The sheet flow deposits merge with the adjacent depositional plains and, in scattered localities, subcrops of a ferruginised sediment occur (Figure 7G). There are two facies of ferruginised sediment. The upper facies (Figure 8F) is a massive, goethite-rich layer that sporadically overlies the lower facies, which contains fine and coarse detrital grains of quartz and plagioclase, indurated by Fe oxides. The ferruginised sediment has formed by cementation of colluvial sand and quartz pebbles, probably sourced from the granitoid, with a lateral accumulation of Fe oxides, possibly from nearby ferruginous bedrock units, such as amphibolites and metabasalts. The regolith developed over amphibolite outcrop is mainly ferruginised bedrock with red lithosols (map unit Sep).

3.4 Depositional plains

Broad colluvial-alluvial depositional plains (Figure 4C) dominate the south and southeast parts of the area. They are generally inclined towards the south. Most of the drainage channels are well defined, generally fringed by dense vegetation (map unit Acaf), with some minor, ill-defined channels or depressions (map unit AOao) which were active where there has been overbank flow. The regolith materials in the channels are a recent alluvium of sand and gravel.

The depositional plains themselves are characterised by extensive areas of black soil (map unit CHpd2; Figure 7F) punctuated by patches of red-brown alluvium with polymictic ferruginous gravel, granules and quartz clasts (map unit CHpd1; Figure 7H). There is sporadic subcrop of underlying lithologies, such as metabasalt, in the black soil plains. On the Landsat imagery (Figure 3), map unit CHpd2 is dominantly greenish-blue hue whereas map unit CHpd1 is blue.

The black soil plains (map unit CHpd2) are characterised by gilgai microrelief caused by shrinking and swelling of smectitic clays. The colour is due to organic matter derived from the grassy vegetation. The soils are commonly 1-2 m thick and are developed on recent colluvium-alluvium overlying Mesozoic saprolite or, in places, Proterozoic lithologies particularly metabasalt that may have partially contributed to their development. They are generally dark brown to black, depending on their physiographic position, with darker coloured soils occupying lower lying areas where smectite can be formed, with high Ca, Mg and Si in the groundwater. The black soils have about 70% in the <75 μm fraction, the remainder being largely quartz grains and pebbles. The <75 μm fraction consist mainly of quartz with smectite, some kaolinite and feldspar. The chemical composition of the <75 μm fraction is given in Table I. Compared to other regolith materials of the Mesozoic and Proterozoic mesas, it is rich in Mn, Mg, Ca and Zr.

Table 1 : Descriptive Statistics of black soils, <75µm fraction (n=8)

Element	Mean	Min	Max	Range	Median	Element	Mean	Min	Max	Range	Median
SiO2 %	62.1	57.2	67.1	9.9	62.1	Ba ppm	456	372	532	160	473
Al2O3 %	14.6	12.5	16.1	3.6	15.0	Zr ppm	403	230	555	325	414
Fe2O3 %	6.4	5.1	8.8	3.8	6.1	Nb ppm	8	<4	17	14	7
MnO %	0.116	0.084	0.165	0.081	0.111	Au ppb	<5	<5	<5	<5	<5
MgO %	1.11	0.78	1.45	0.67	1.19	Ce ppm	105	79	158	79	93
CaO %	0.66	0.42	1.00	0.58	0.58	Cs ppm	4	3	5	2	4
Na2O %	0.44	0.24	0.66	0.42	0.42	Eu ppm	2.3	1.7	4.6	2.9	2.1
K2O %	0.96	0.70	1.21	0.51	0.97	Hf ppm	11.0	6.3	16.0	9.7	11.1
TiO2 %	0.9	0.8	1.0	0.2	0.9	Ir ppb	7	7	7	0	7
P2O5 %	0.06	0.04	0.09	0.04	0.05	La ppm	48.6	33.9	80.8	46.9	43.5
LOI %	8.2	6.7	9.1	2.4	8.3	Lu ppm	0.8	0.6	1.3	0.7	0.7
Cr ppm	63	52	73	21	63	Rb ppm	66	48	79	31	68
V ppm	142	93	226	133	139	Sm ppm	10.4	7.7	15.4	7.7	10.0
Cu ppm	20	12	31	19	20	Sc ppm	14.6	12.7	16.3	3.6	14.7
Pb ppm	21	14	27	13	21	Se ppm	<5	<5	<5	<5	<5
Zn ppm	67	41	92	51	71	Ta ppm	1.651	1	2	1	2
Ni ppm	67	25	143	118	54	Th ppm	16.9	11.2	30.5	19.3	14.9
Co ppm	21	12	38	26	20	Yb ppm	5.4	3.9	9.1	5.2	5.1
As ppm	7	4	14	9	6	Br ppm	5	2	9	7	5
Sb ppm.	0.4	0.3	0.5	0.2	0.4	Sr ppm	143	116	212	96	132
Mo ppm	<5	<5	<5	<5	<5	U ppm	<2	<2	3	3	<2
Ag ppm	<5	<5	<5	<5	<5	Y ppm	49	33	90	57	43
Ga ppm	18	15	21	6	17	Cl ppm	<20	<20	<20	<20	<20
W ppm	<2	<2	<2	<2	<2	S ppm	159	120	190	70	165

FIGURE 7

REGOLITHS AND LANDFORMS

A. Lateritic nodules on top of mesa developed on Mesozoic sediments. Associated with map unit DFls. AMG 483130 mE, 7581270 mN, Zone 54K.

B. Erosional escarpment on Mesozoic sediment. The brecciated Fe-stained and mottled silicified saprolite contains siliceous breccia formed by the collapse of the saprolite through removal of the clay matrix by leaching. Associated with map unit See. AMG 482990 mE, 7581480 mN, Zone 54K.

C. Pediment around Mesozoic mesa with deeply incised gullies and covered dominantly by a veneer of silicified saprolite fragments. The ochre stains (1) are due to underlying goethitic layers which represent redox zones or associated with more permeable layers within the sediment pile. The pale to brownish saprolitic clays are smectitic and are readily erodible. Associated with map unit Sei2. AMG 483250 mE, 7581550 mN, Zone 54K.

D. Megamottles (1) in brecciated Fe-stained and mottled silicified saprolite (2) on Mesozoic sediments. Associated with map unit See. AMG 482160 mE, 7580600 mN, Zone 54K.

E. Colluvial outwash on pediment of Mesozoic mesa. It consists of a veneer of polymictic Fe-rich gravels, quartz gravels and silicified and brecciated siltstone fragments. Associated with map unit CHei1. AMG 483680 mE, 7584600 mN, Zone 54K.

F. Black soil on depositional plain. The black soil is smectitic, generally 1 - 2 m thick, and contains quartz gravels and lithic fragments. Gilgai microrelief is common. Associated with map unit CHpd2. The view is from AMG 481900 mE, 7584840 mN, Zone 54K.

G. A scattering of ferruginised sediment fragments (1) on a colluvial-alluvial plain. The ferruginised sediment consists of coarse sand with quartz pebbles indurated by Fe-oxides. The sediment occurs at the basal unconformity between the Mesozoic and Proterozoic. Associated with map unit CHei2. AMG 482460 mE, 7588900 mN, Zone 54K.

H. Red-brown sheetflow deposit on depositional plain. The sheetflow deposit contains red-brown alluvium, polymictic ferruginous granules and gravels and quartz clasts. Associated with map unit CHpd1. AMG 469900 mE, 7587900 mN, Zone 54K.

A

B

C

D

E

F

G

H

FIGURE 7 (cont'd)

REGOLITHS AND LANDFORMS

I. Fragments of hematite after magnetite (1) on flanks of Proterozoic granitic hill. The top of the hill is covered with remnant Mesozoic sediments (2). The hematite-rich vein is related to the late-stage hydrothermal activity associated with granite emplacement. (Refer Figure 8H). AMG 475490 mE, 7588670 mN, Zone 54K.

J. The unconformity between Mesozoic sediments and Proterozoic basement. This unconformity is a ferruginised sediment of coarse sand with pebbles (1). Granite saprolite is in the lower right of the picture (2), with silicified, pale, Mesozoic siltstones above (3). AMG 478380 mE, 7590800 mN, Zone 54K.

K. Sheetflow deposits of red colluvial-alluvial sands on pediments of Proterozoic granitic hills. Associated with map unit CHei2. The view is SSE from AMG 469300 mE, 7588970 mN, Zone 54K.

L. The sheetflow deposits (1) similar to Figure 7K can be as thick as 1 m overlying granite (2). AMG 480900 mE, 7589030 mN, Zone 54K.

M. The polymictic lag on a pediment at the Tringadee Prospect. It consists of fragments of ferruginous bands which are goethite-manganese rich (1) or goethite stained (2). Associated with map unit Sei1. AMG 479600 mE, 7579800 mN, Zone 54K.

N. View of Brumby Prospect which lies on low hills of Mesozoic sediment. AMG 475400 mE, 7584430 mN, Zone 54K.


I
2
1


J
3
1
2


K

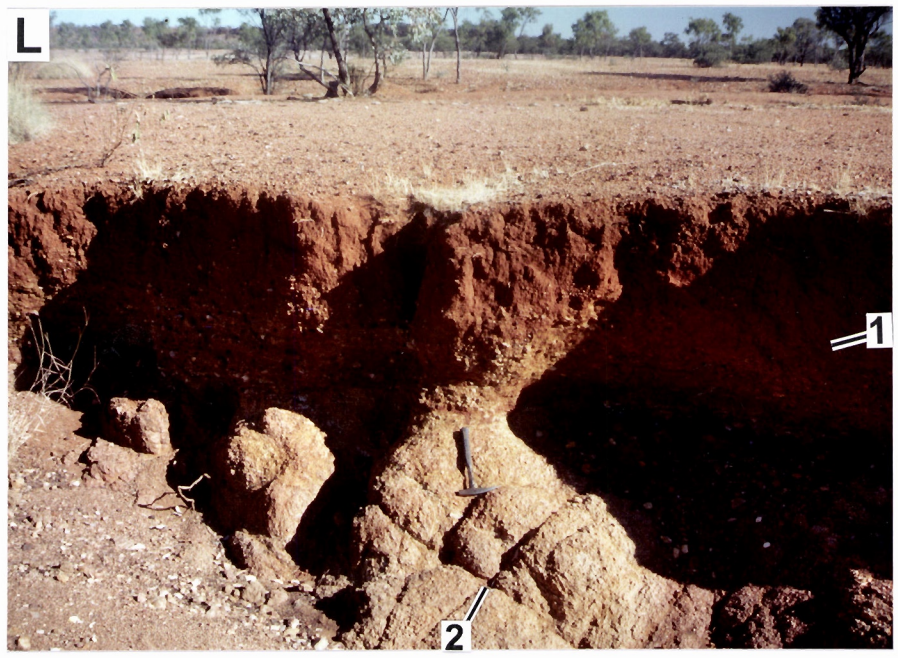
L
1
2


M
1
2


N

FIGURE 8

REGOLITH MATERIALS

A. A lateritic nodule developed in Mesozoic siltstone. The Fe oxides are mainly hematite and goethite and occur as vermiform coatings on the lateritic nodule (1) or as infillings in cracks (2) in the silicified, kaolinitic breccia (3). Photomicrograph in normally reflected light. Specimen TG 72 : AMG 482990 mE, 7581480 mN, Zone 54K.

B. A silicified, mottled duricrust that consists mainly of goethite and kaolinite. Specimen TG 73 : AMG 482990 mE, 7581480 mN, Zone 54K.

C. Close up of a brecciated silicified saprolite. The coarse Fe-stained silicified clasts (1) form a skeleton in which smaller angular clasts (2) fill the interstitial spaces. The Fe tends to be leached from the edges of the angular clast (3). Other clasts (4) are more strongly leached. Specimen TG 502 : AMG 482990 mE, 7581480 mN, Zone 54K.

D. Lateritic duricrust developed on Proterozoic granite. It consists of cemented pisoliths cored either with a quartz grain (1), hematite (2) or a conglomerate of hematite and kaolinitic clay spherules (3). Photomicrograph in plain polarised light. Specimen TG 204 : AMG 469120 mE, 7589130 mN, Zone 54K.

E. Goethite and Mn-rich band that has scavenged Zn (2145 ppm). It also contains quartz, kaolinite and mica. Specimen TG 147 : AMG 483290 mE, 7582740 mN, Zone 54K.

F. Ferruginised sediment. This massive, goethite-rich facies shows different generations of goethite growth layers. It commonly occurs patchily over a lower facies of ferruginised sediment that contains more fine and coarse grains of quartz and plagioclase. Specimen TG 504/1 : AMG 482370 mE 7588970 mN, Zone 54K

G. An example of sub-vertical ferruginous vein found at the Brumby Prospect. It consists dominantly of hematite, goethite, kaolinite and quartz. Specimen TG 103 : AMG 475050 mE, 7584600 mN, Zone 54K.

H. Hematite-rich vein emplaced in granite. The hematite has trellis structures (1) indicating derivation from magnetite. It also contains fractures (2). Photomicrograph in normally reflected light. Specimen TG 189 : AMG 476270 mE, 7589310 mN, Zone 54K.

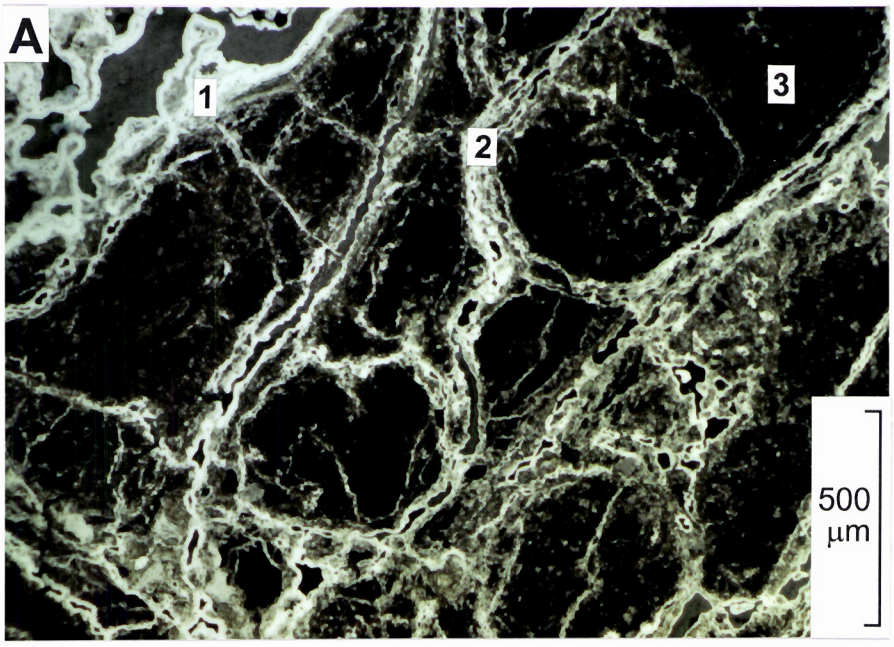
A
1
2
3
500
µm


B
1 cm

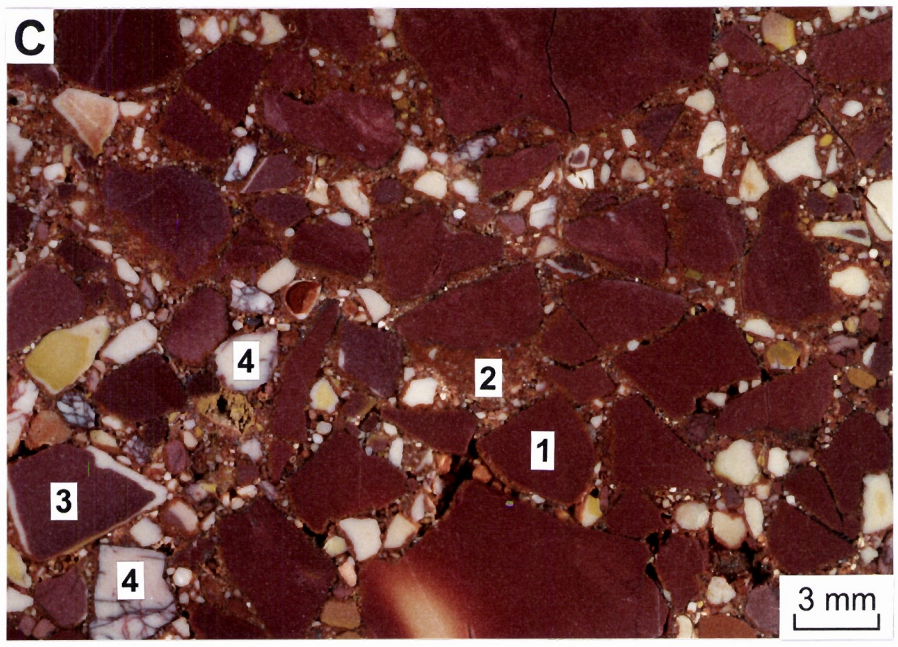
C
4
2
1
3
4
3 mm

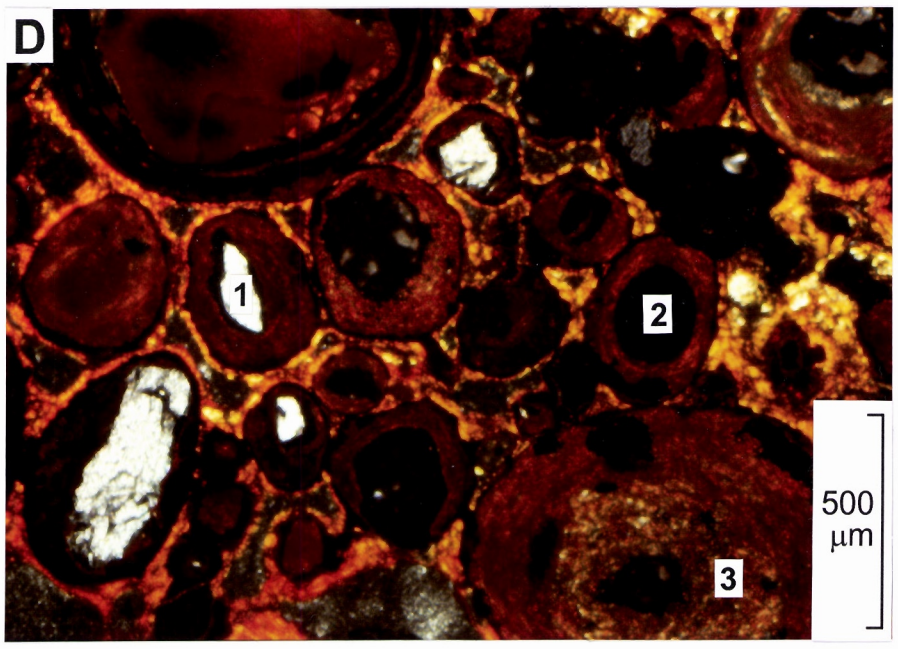
D
1
2
3
500
µm


E
1 cm


F
1 cm


G
1 cm

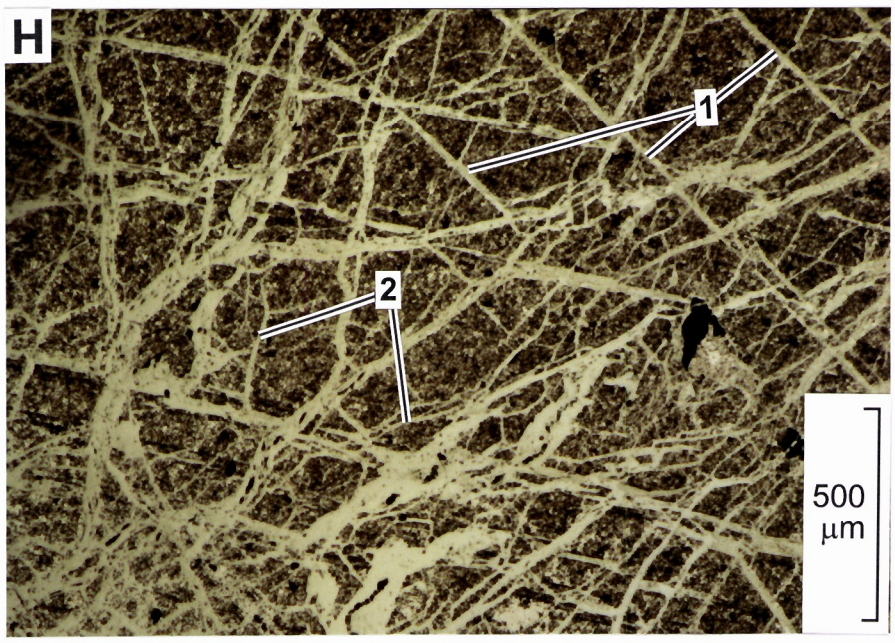
H
1
2
500
µm

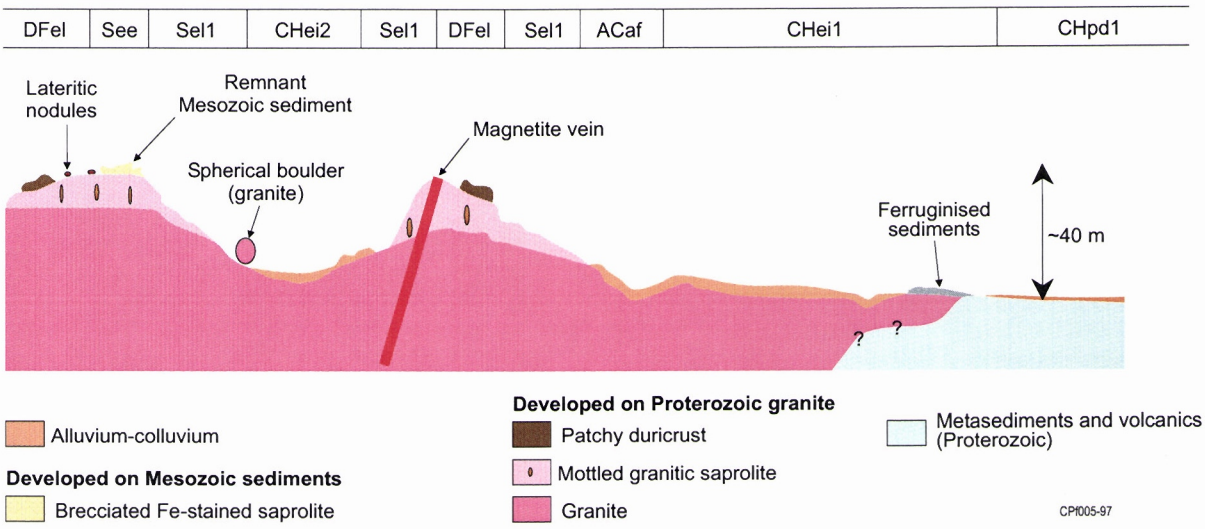

Figure 9. Regolith-landform units on Proterozoic granitoids.

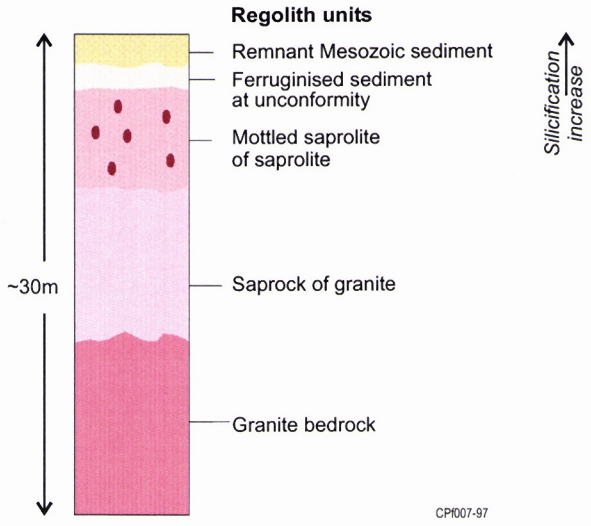

Figure 10. Schematic vertical section through weathering profile over granitoid.

4. TRINGADEE Zn PROSPECT

The Tringadee prospect lies on the pediment of the Mesozoic hills and is covered with a polymictic lag of goethite and Mn rich lithic fragments and Fe-stained brecciated, silicified saprolite, associated with map unit Sei1 (Figure 7M). There is a widespread Zn anomaly of >1000 ppm (Figure 2) in the Mesozoic cover which is confined to a north-striking palaeovalley, but is isolated from Cannington Pb-Zn-Ag deposit by a palaeohigh. This is a feature interpreted from drilling. The source of the Zn at Tringadee is unknown. Representative sections showing the nature of the regolith and the location of the Zn anomaly are shown in Figure 11. The Mesozoic cover varies from 20 to 30 m thick, with underlying Proterozoic granite.

As part of a more detailed study to explain the Zn anomaly, two RAB drill intersections at Tringadee prospect (ROTR 155 at 479500 mE - 7580000 mN and ROTR 156 at 479500 mE - 7580000 mN) with a Zn anomaly of >1000 ppm were investigated. This RAB drilling lies on the alluvial-colluvial plains near exposures of low mounds of Fe and Mn oxide-rich Mesozoic sediments (prominent ochre colour on aerial photos). Dating of Mn oxides on surface sample TG147 (483288 mE 7582737 mN) by Vasconcelos (1998), using $^{40}Ar/^{39}Ar$ analysis, indicates a probable late Miocene age of 12 Ma. Similar ages were also obtained from Mn samples from the Cowie and Pegmont prospects. A schematic regolith profile of ROTR 156, showing the dispersion of Zn and related elements, is given in Figure 12. Profile ROTR 155 (not shown here) has similar element distributions.

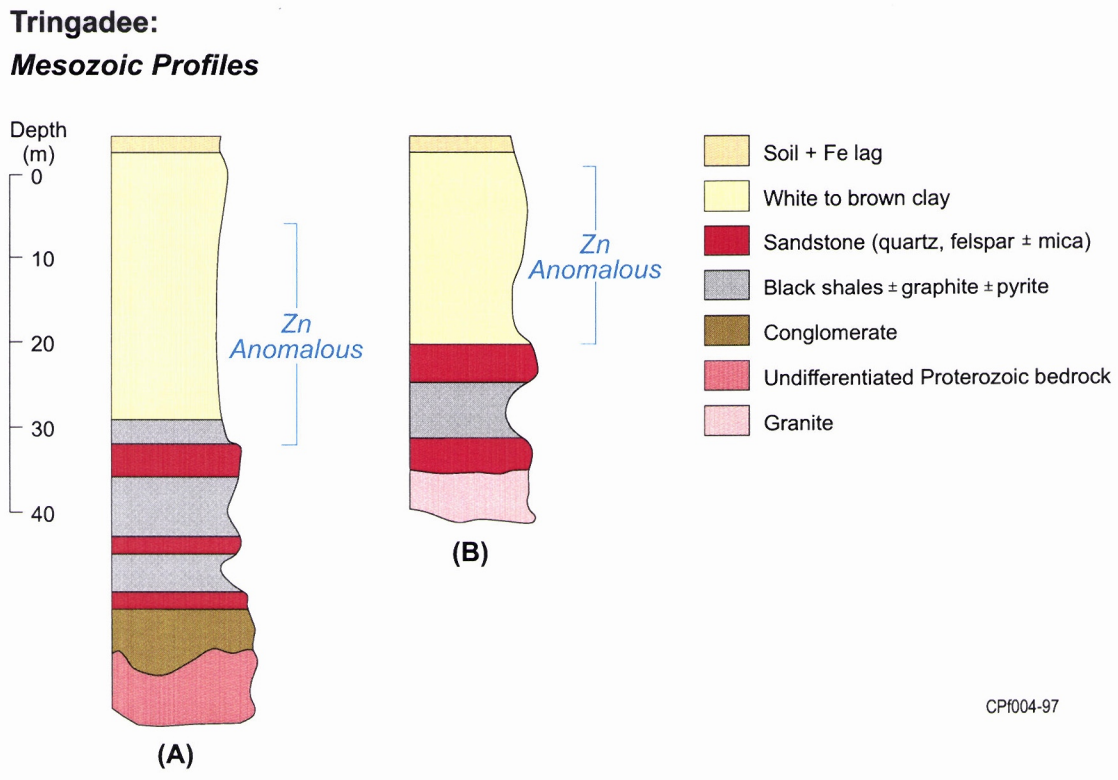

Figure 11. Section through the Mesozoic sediments at the Tringadee Prospect showing anomalous Zn (Aberfoyle Resources Ltd). (A) represents profile in RAB line 479200-480200 mE 7580000 mN, of which ROTR 155 and 156 are located. (B) is an adjoining line which represents profile in RAB line 479000 - 480000 mE 7581100 mN.

The size fraction of samples collected from drill intersections ROTR 155 and 156 that gives the best geochemical signature of the pathfinder elements was investigated by a geochemical orientation study. Based on the median values for the concentration of Zn, Cu, Pb, As and Sb, the >2000 μm and 710-2000 μm fractions give comparable values (as shown in boxes in Table 2). They contain variable amounts of Fe (2-60% Fe_2O_3), Al (6-20% Al_2O_3) and Si (22-70% SiO_2). Methods of geochemical and mineralogical analyses are given in Appendix II.

From this information, together with the practicality of obtaining enough material, the >710 μm fraction was selected for further analysis. When this was insufficient, the <710 μm fraction, which is dominated by quartz and kaolinite, was used instead. Samples at various depths within a profile were selected for analyses based mainly on colour change. For ferruginous bands in the saprolite, the >710 μm fraction was separated into Mn-rich and Fe-rich materials. Complete geochemical data for ROTR 155 and 156 are given in Tables A2 and A3 in Appendix III.

Zinc is relatively enriched in subsurface ferruginous bands at depths of 5-10 and 20-25 m, where the concentration of Fe_2O_3 reaches 60%. The 20-25 m interval contains goethite with dendritic overgrowths of hollandite. The Zn content of the ferruginous bands is 1300-2000 ppm compared to <200 ppm in the clay-rich materials. Copper is also enriched, to a maximum of 170 ppm. Lead concentrations are low in both fine and coarse fractions but reach up to 200 ppm in two Mn-rich samples. The As contents vary from 1 to 51 ppm, with the high concentrations associated with Fe-rich samples. Goethite and hollandite are most likely hosts for elements that are mobilised during weathering.

From these data and observations of RAB geochemical data from Aberfoyle Resources Ltd, it appears the Zn anomaly in the Mesozoic cover is associated with accumulated Fe and Mn oxides. Zinc appears to be more closely correlated to Fe than Mn, but where Fe is associated with high Mn, Zn is increased to >1000 ppm. However, low contents of Pb, which is relatively less mobile, suggests a distal source. The Tringadee area is interpreted to have remained in a low part of the landscape before, during and after deposition of the Mesozoic sediments. Iron, Mn and Zn appear to have derived from external sources and have migrated laterally along permeable layers, precipitating at redox fronts within the sediment pile. This probably occurred after deposition, but contemporaneous accumulation of the metals with the sediments is possible. In conclusion, it is considered that the source of the Zn is external and that it has been scavenged by Fe-Mn oxide precipitates, now represented by ferruginous bands. There is thus no relationship between Zn anomalies in the sedimentary cover and potential base metal mineralisation in the basement.

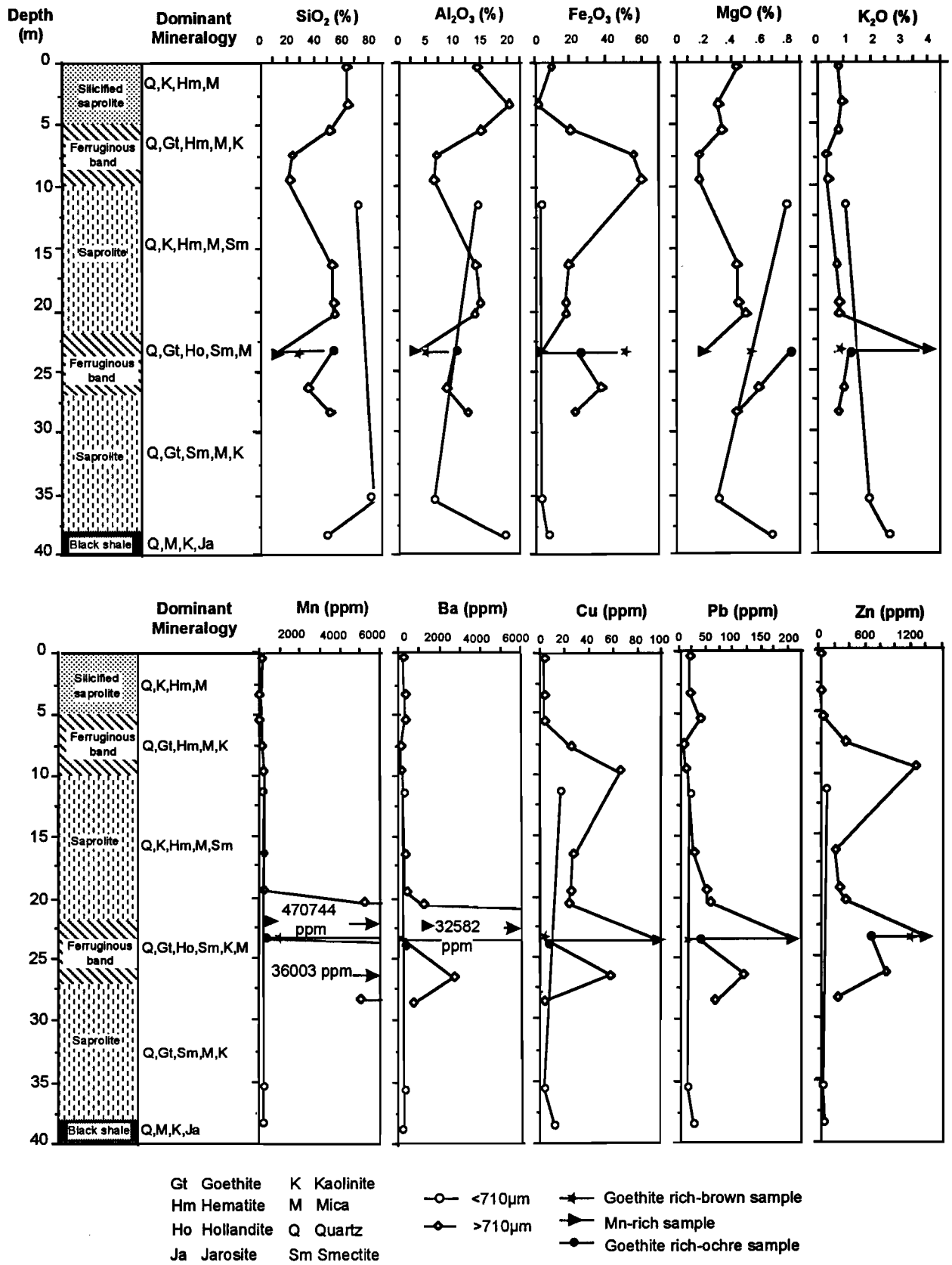

Figure 12. Schematic regolith profile for RAB ROTR156 showing the distribution of certain major and trace elements, Tringadee Prospect.

Table2
Tringadee : geochemical orientation study data

Sample No	Depth	Size	Element	SiO2	Al2O3	Fe2O3	MgO	CaO	Na2O	K2O	TiO2	P2O5	MnO	LOI	Cr	V	Cu	Pb	Zn	Ni	Co	As	Sb	Mo	Ag
	(m)	fraction	Unit	%	%	%	%	%	%	%	%	%	%	%	ppm	ppm	ppm	ppm	ppm	ppm	ppm	ppm	ppm	ppm	ppm
		(µm)	Detection Limit	0.01	0.01	0.01	0.01	0.001	0.01	0.001	0.001	0.001	0.001		5	5	10	5	20	10	1	1	0.2	5	5
			Method	XRF	XRF	XRF	XRF	XRF	XRF	XRF	XRF	XRF	XRF		NAA	XRF	XRF	XRF	XRF	XRF	NAA	NAA	NAA	NAA	NAA
ROTR155																									
TG20A	19.5	>2000		24.88	6.42	47.44	0.52	0.13	0.12	1.06	0.31	0.548	5.914	10.21	30.5	184	114	111	2061	915	1030	22.4	0.45	<5	<5
TG20B	19.5	710-2000		28.47	6.77	43.05	0.50	0.15	0.11	1.09	0.33	0.567	5.814	9.91	30.2	198	135	117	1791	748	916	23.3	0.66	<5	<5
TG20F	19.5	<75		62.73	13.88	8.51	1.41	0.39	0.23	1.65	0.64	0.136	0.068	6.85	53.5	145	22	12	421	126	49.6	5.25	0.23	<5	<5
TG23A	22.5	>2000		26.84	6.54	47.48	0.52	0.11	0.09	0.88	0.31	0.363	3.294	9.75	25.8	98	31	10	1696	588	649	15	<0.2	<5	<5
TG23B	22.5	710-2000		27.84	6.67	45.72	0.52	0.11	0.10	0.85	0.32	0.400	3.155	9.61	24.7	112	34	29	1640	659	800	15.1	0.32	<5	<5
TG23F	22.5	<75		63.80	13.19	8.58	1.31	0.31	0.21	1.69	0.63	0.086	0.051	6.35	51.1	134	<10	10	309	111	33.9	4.66	<0.2	<5	<5
ROTR156																									
TG43A	9.5	>2000		21.91	6.69	59.76	0.17	0.05	0.05	0.41	0.35	0.812	0.033	10.28	59.1	326	65	12	1255	415	104	38.3	0.88	<5	<5
TG43B	9.5	710-2000		19.00	5.87	60.61	0.14	0.09	0.05	0.36	0.31	0.879	0.037	10.64	58.5	336	105	38	1243	385	97.8	36.9	0.65	<5	<5
TG43F	9.5	<75		63.06	16.08	8.06	0.67	0.31	0.11	1.07	0.74	0.113	0.011	7.45	56.8	138	30	17	201	92	17	5.68	0.28	<5	<5
TG54A	20.5	>2000		55.28	14.16	17.08	0.51	0.16	0.12	0.85	0.63	0.250	0.667	8.27	45.1	199	23	56	342	150	111	16.4	0.42	<5	<5
TG54B	20.5	710-2000		38.50	9.86	34.77	0.50	0.15	0.12	0.89	0.46	0.498	1.904	9.24	42	223	59	73	928	346	323	27.8	0.54	<5	<5
TG54F	20.5	<75		64.18	13.66	7.51	1.31	0.37	0.26	1.64	0.62	0.142	0.028	6.58	50.6	140	13	13	322	110	26.6	7	0.36	<5	<5

Table2 (con'td)
Tringadee : geochemical orientation study data

Element	Ga	W	Ba	Zr	Nb	Au	Ce	Cs	Eu	Hf	Ir	La	Lu	Rb	Sm	Sc	Se	Ta	Th	Yb	Br	Sr	U	Y	Cl	S
Unit	ppm	ppm	ppm	ppm	ppm	ppb	ppm	ppm	ppm	ppm	ppb	ppm	ppm	ppm	ppm	ppm	ppm	ppm	ppm	ppm	ppm	ppm	ppm	ppm	ppm	ppm
Detection Limit	3	2	30	5	4	5	2	1	0.5	0.5	20	0.5	0.2	5	0.2	0.1	5	1	0.5	0.5	2	5	2	5	20	10
Method	XRF	NAA	XRF	XRF	XRF	NAA	NAA	NAA	NAA	NAA	NAA	NAA	NAA	XRF	NAA	NAA	NAA	NAA	NAA	NAA	NAA	XRF	NAA	XRF	XRF	XRF
ROTR155																										
TG20A	9	<2	1402	55	<4	<5	44.4	10.8	1.15	1.56	<20	12.7	0.41	57	4.61	11.5	<5	<1	4.7	2.94	<2	48	<2	21	<20	170
TG20B	12	<2	2821	68	<4	<5	51.9	11.6	1.44	1.81	<20	16.3	0.39	60	5.35	11.1	<5	<1	4.91	2.84	<2	98	<2	26	10	420
TG20F	17	<2	226	118	<4	<5	43.6	17.5	1.07	3.24	<20	21	0.33	116	4.68	13.5	<5	1.11	8.2	2.38	10.8	69	<2	25	100	240
TG23A	7	<2	4928	66	<4	<5	36.9	10.2	0.94	2.35	<20	10.7	0.32	65	3.62	7.61	<5	1.63	4.15	2.28	<2	28	<2	18	<20	110
TG23B	9	<2	4629	62	<4	<5	43.4	9.22	1.02	1.55	<20	11.5	0.34	62	3.88	7.47	<5	1.31	4.39	2.57	<2	34	<2	20	<20	170
TG23F	17	<2	263	139	<4	<5	36.7	11.9	0.72	3.65	<20	19.3	0.28	102	3.53	11.7	<5	<1	8.4	2.06	3.05	47	<2	18	10	290
ROTR156																										
TG43A	14	<2	108	66	<4	<5	21.8	8.22	1.37	1.79	<20	9.44	0.87	37	5	41.8	<5	1.13	7.33	5.75	2.48	38	4.4	25	<10	960
TG43B	10	<2	76	53	<4	<5	16.8	7.24	1.59	1.58	<20	7.65	0.93	28	4.81	45.4	<5	<1	6.59	6.03	<2	29	7.81	31	30	1160
TG43F	18	<2	196	137	<4	<5	45.8	5.44	1.18	4.02	<20	21.2	0.36	58	4.71	18.2	<5	<1	8.15	2.69	<2	112	<2	17	10	620
TG54A	18	<2	1231	117	<4	<5	72.8	4.8	1.13	3.32	<20	30	0.3	44	4.86	15.8	<5	<1	8.28	2.49	<2	167	<2	17	<20	510
TG54B	12	<2	3215	94	<4	<5	87.7	8.46	1.69	2.41	<20	26.8	0.48	56	6.75	19.3	<5	1.85	6.69	3.74	2.02	145	<2	30	30	920
TG54F	19	<2	320	116	<4	<5	47.5	13.6	1.3	3.23	<20	23.4	0.33	101	5.33	13.3	<5	<1	8.05	2.68	4.6	62	<2	23	<20	260

5. BRUMBY Cu-Au PROSPECT

The Brumby Cu-Au prospect is situated in low hills of Mesozoic cover (Figure 7N) over steeply-dipping Proterozoic bedrock. Hydrothermal mineralisation in the Proterozoic contains magnetite, chalcopyrite and gold (verbal communication with Aberfoyle Resources). A stratigraphic relationship through the regolith at Brumby is given in Figure 13.

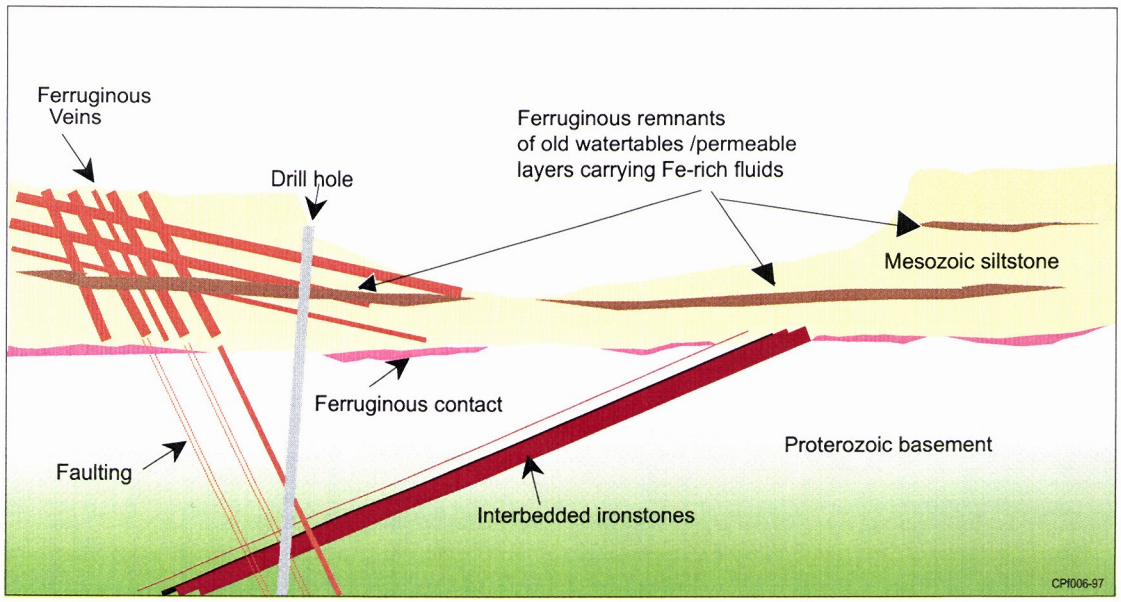

Figure 13. Stratigraphic relationship of the Brumby Prospect.

There are two main types of ferruginous materials in the area, namely, surface ferruginous veins and subsurface ferruginous bands. The surface ferruginous veins are structurally controlled and probably follow tectonically-induced cross-cutting fracture systems in the Mesozoic. They consist largely of hematite, goethite, kaolinite and quartz. Goethite tends to increase with depth. Figure 8G shows an example of a ferruginous vein. The sub-surface ferruginous bands are sub-horizontal and represent either redox zones or preferred pathways for induration by Fe-rich fluids in the more permeable layer of the sediments. They consist dominantly of goethite and / or Mn oxides-rich.

The focus of the study was to assess if these ferruginous veins and ferruginous bands in the Mesozoic sediments could indicate concealed mineralisation.

Eleven samples of surficial ferruginous veins were studied along transect 7584400 mN running from 474000 to 475500 mE over minor mineralisation drilled by Aberfoyle Resources Ltd. Bulk geochemical analyses of the surficial ferruginous veins (Table A4 in Appendix III) using methods given in Appendix II, showed Au below detection limits (5 ppb) and low contents of Cu (50 ppm). Partial extractions did not show any increase in contrast of gold or copper and therefore did not augment bulk analysis information

Selected sub-surface samples were chosen from a cluster of RAB drill holes around a percussion drill hole (PETD6). All contain less than 50 ppm Cu in the 15 m of Mesozoic drilled (Aberfoyle Resources Ltd unpublished data). The Mesozoic is approximately 45 m thick at this point. Zinc increases in the top ten metres, showing an accumulation that is unrelated to mineralisation. No

analyses for Fe or Au were done by Aberfoyle Resources Ltd on the RAB samples, so no evaluation of deeper ferruginous bands in the Mesozoic could be made. Twenty additional samples were submitted for multi-element analysis from 0 to 55 m of mineralised percussion intersection PETD6 (Table A5 in Appendix III; Figure 14). These showed a strong Fe accumulation at the Proterozoic-Mesozoic boundary at 45 to 50 m depth. This may be related to a preferred pathway for solutions and perhaps a perched aquifer. Copper, Zn and other trace elements increase around the Mesozoic-Proterozoic boundary. At 25 m, there is a ferruginous band which represents either a redox zone or a permeable layer in the sediment pile (conduit for Fe-rich fluids) where Cu and Zn have accumulated. Below 25 m, Fe, Au and Cu correlate well but above 25 m the correlation between Au and Cu, and Au and Fe is less. Copper becomes increasingly depleted towards the surface decreasing from a maximum of 8000 ppm in the Proterozoic to 400 ppm at 25 m and 40 ppm at the surface.

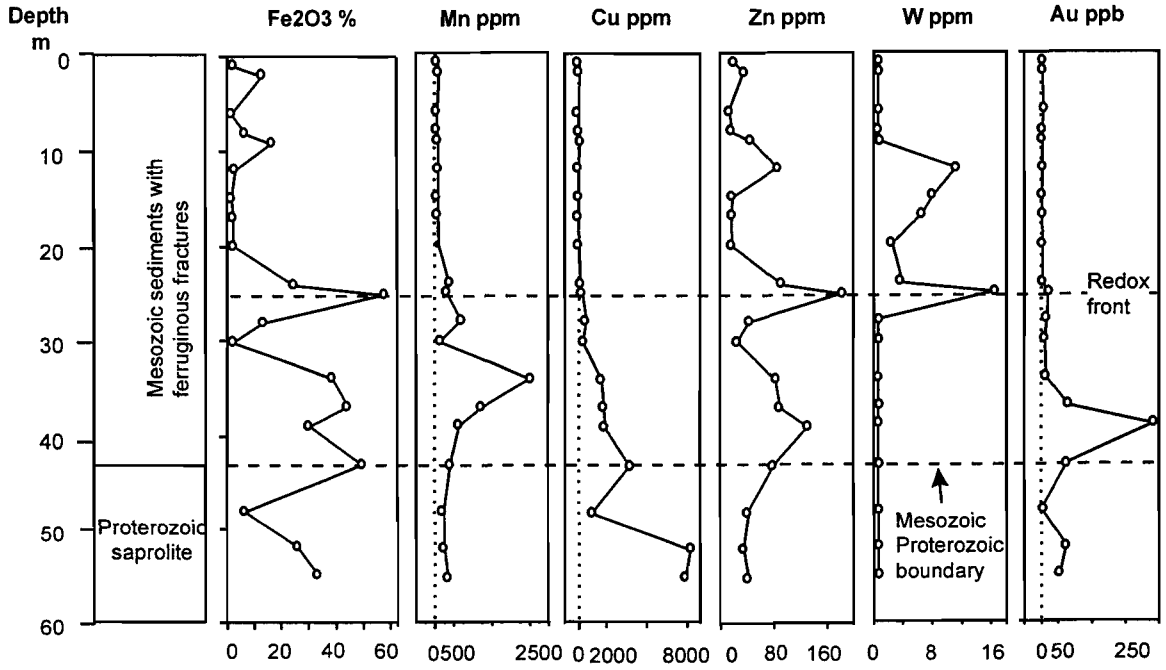

Figure 14. Brumby Prospect percussion drill hole PETD6

In conclusion, there is no expression of mineralisation in the structurally controlled surficial ferruginous veins in the Mesozoic at Brumby. Hydromorphic dispersion of Cu, Zn and Au, around the ferruginous bands at Proterozoic-Mesozoic boundary (45 to 50 m depth) and at 25 m accumulate Cu, Zn and Au which are related to underlying mineralisation.

6. REGOLITH EVOLUTION

The Mesozoic sediments are flat lying and unmetamorphosed; the region has been part of a relatively stable tectonic block (Blake, Jaques and Donchak, 1983). The sedimentary unit that is most extensive is the Gilbert River Formation, which consists of poorly sorted, cross-bedded, sandstone and conglomerate, in the lower part of the formation and siltstone in the upper part. Blake et al (1983) stated that late in the Cretaceous or early Tertiary, the region was gently uplifted, initiating the most recent geologic cycle of weathering, erosion and deposition.

It is postulated that, during the period of gentle uplifting, ferruginisation and silicification overprinted each other. Lateritic weathering of the Mesozoic sediments formed mottles and lateritic duricrust. Iron may have been derived laterally or from ferruginous veins emplaced in the granite during late-stage hydrothermal activity. Silicification has impregnated more permeable parts of the lateritic profile. At times of intense leaching, movement of clay out of less silicified parts of the weathering profile resulted in a brecciated Fe-stained silicified saprolite. Formation of the collapsed saprolite and differential erosion of the Mesozoic sediments, related to differences in silicification or ferruginisation is probably responsible for the variety of heights of the sediment capped mesas. The present Mesozoic mesas on granite in the north can be about 100 m higher than those in the south. This variation in topography is reflected by the present main drainage (Bustard creek) which flows south. It is unclear if deep weathering of the granitoid occurred prior to Mesozoic sedimentation, although this is unlikely (Li Shu and Robertson, 1997). The sediments were deposited over an undulating topography which has, in turn, controlled the dispersion of elements.

Goethite and Mn oxide-rich bands occur at the base of the mesas. Some of these bands form steplike microrelief. These ferruginous bands reflect past redox zones or permeability contrasts within the sediments associated with cyclical sedimentation. Goethite and Mn oxides in these bands have scavenged Zn and other trace elements, so forming the Zn anomaly at the Tringadee Prospect in the Mesozoic cover. The source of the Zn anomaly is likely to be external. Gentle uplifting also resulted in fractures in the Mesozoic forming conduits for fluids rich in Fe. These are common at the Brumby Prospect where ferruginous veins crisscross each other.

7. IMPLICATIONS FOR EXPLORATION

The Tringadee prospect is interpreted to have remained in a low part of the landscape before, during and after deposition of Mesozoic sediments. It is considered that the source of the Zn is external and that it has been scavenged by Fe-Mn oxide precipitates, now represented by ferruginous bands.

The Brumby prospect shows that structurally controlled, subvertical, ferruginous veins in the Mesozoic give little indication of mineralisation. In contrast, ferruginous bands associated with redox zones or permeability layers within the sediment pile have accumulated trace elements related to underlying mineralisation.

For reconnaissance, ferruginous bands should be preferentially collected as sampling media but careful interpretation of data is needed. The inclusion of Fe, Mn and Pb in the analytical suite enhances data interpretation. Copper and Zn anomalies associated with high Pb concentrations may suggest the proximity of a base metal mineralisation. Different thresholds for Zn and Cu have to be used particulary where there is enrichment in Mn and Fe-oxides.

8. ACKNOWLEDGEMENTS

Assistance from Aberfoyle Resources Limited was by P. Komyshan, E. Dronseika, D. Hicks and K. Mathews. Later, S. Konecny of BHP Minerals assisted at Tringadee. Thin and polished sections were prepared by R.J. Bilz. Geochemical analyses were by M.K.W. Hart (XRF) at CSIRO and Becquerel Laboratories (INAA) at Lucas Heights. AAS analysis was done by K.A. Howe. Sample preparation was by S. L. Keppler and K. Lim. X-ray diffraction analysis was by M.K.W. Hart. Artwork was provided by A.D. Vartesi and T.R. Naughton supervised by C.R. Steel. R.R. Anand, I.D.M. Robertson and C.R.M. Butt provided critical review of the manuscript. All this assistance is acknowledged with appreciation.

9. REFERENCES

Blake, D.H., Jaques, A.L. and Donchak, P.J.T. 1983. Selwyn region, Queensland, 1:100,000 Geological map commentary, BMR, Australia, 29pp.

Li Shu and Robertson, I.D.M. 1997. Surficial geology around the Eloise Cu-Au mine and dispersion into Mesozoic cover from the Eloise Mineralisation, N.E. Queensland. CRC LEME Report 56R/CSIRO Exploration &Mining Report 405R, 72pp.

Vasconcelos, P. 1998. Geochronology of weathering in the Mount Isa and Charters Towers regions, Northern Queensland. CRC LEME Restricted Report 68R.

APPENDICES

Appendix I

Map : Tringadee Area Regolith Landforms (1:50,000 scale)

APPENDIX II

METHODS OF GEOCHEMICAL AND MINERALOGICAL ANALYSES

Geochemical Analysis
All samples were analysed by XRF (CSIRO) and INAA (Becquerel Laboratories), as follows:-

Neutron activation analysis (INAA): 10 g aliquots in plastic vials were analysed for Ag, As, Au, Br, Ce, Co, Cr, Cs, Eu, Hf, Ir, La, Lu, Mo, Sb, Sc, Se, Sm, Ta, Th, U, W, Yb.

X-Ray fluorescence on fused discs (XRF(f)): 0.7 g of sample were fused with 6.4 g Li borate and analysed using a Philips PW 1480 by the method of Norrish and Hutton (1969) : Si, Al, Fe, Mg, Ca, Na, K, Ti, P, Mn, Ba, Cl, Cu, Ga, Ni, Nb, Pb, Rb, S, Sr, Ti, V, Y, Zn, Zr.

Partial Extraction:
In a centrifuge, 1.2 g of sample were shaken and suspended in 40 ml ammonium citrate solution at pH 7.0; 0.25g of sodium dithionate were added and left in ultrasonic waterbath at 80^0C for one hour. The sample was centrifuged and the supernatent extracted. This procedure was repeated another two times with 0.25 g sodium dithionate and two more times with 0.5 g sodium dithionate as the high-iron samples were very resistant to the reducing agent in neutral conditions. The combined supernatent solutions were boiled down in beakers on a hotplate and digested with aqua-regia and finally made up to 50 ml with 0.2 M HCl. Solutions were sent for Atomic absorption spectrophotometry and 20 mls was dried onto 2 g of carbon and sent for INAA.

Mineralogical Analysis
X-Ray diffraction: Selected samples were examined by XRD using a Philips PW1050 diffractometer, fitted with a graphitè crystal diffracted monochromator and CuKα radiation. Each sample was scanned over the range 2-65^0 2θ at a speed of 0.5 ^{0}/min.

Petrological studies : Polished blocks were made of samples with Fe-rich materials and observed under normally reflected light. Thin sections were made for selected samples.

Appendix III

Table A1: Geochemistry of regolith materials

Table A2: Geochemistry of RAB drill hole ROTR 155 at Tringadee Prospect

Table A3: Geochemistry of RAB drill hole ROTR 156 at Tringadee Prospect

Table A4: Geochemistry of ferruginous veins at Brumby Prospect

Table A5: Geochemistry of percussion drill hole PETD 6 at Brumby Prospect

Table A1 : Geochemistry of regolith materials (XRF fusion method).

			Mesozoic siltstone lithology										Proterozoic granitoid lithology			
Sample no			TG72	TG74	TG73	TG502	TG75	TG79	TG128F	TG129F	TG130F	TG147	TG-204	TG-205	TG-189	TG511
Description			Lateritic nodules	Lateritic nodules	Mottled duricrust	Brecciated silicif'd saprolite	Silicified saprolite	Grey white saprolite clay	White saprolite clay(<75µm)	Purplish saprolite clayl(<75µm)	Brown saprolite clayl(<75µm)	Goethite-Mn band	Ferruginous duricrust	Lateritic nodules	Magnetite vein	Granite saprock
Dominant minerals			Hm,K,Gt,Q	Gt,K,Q,Hm	Gt,K,Q,Hm	Q,Op	Q,Op,K,Hm	K,Q,Sm,F	Q,K,Sm	Q,K,Sm,Gt	Q,K,Sm	Gt,Ho,Li	Gt,Q,Hm	Gt,Q,Hm	Hm,Gt	Q,F,M
Northing			7581477	7581477	7581477	7581477	7581477	7581477	7581467	7581467	7581467	8E+06	7589130	7589130	7588500	7589310
Easting			482988	482988	482988	482988	482988	482988	483114	483114	483114	483288	469115	469115	476267	481881
Element	Unit	Det. limit														
SiO2	%	0.01	23.17	29.42	40.28	83.55	75.90	66.80	63.04	56.73	59.80	20.9	23.00	15.91	2.81	72.38
Al2O3	%	0.01	14.54	16.66	13.48	2.84	8.39	14.44	21.65	19.23	21.29	5.45	14.22	12.00	0.51	15.3
Fe2O3	%	0.005	52.38	42.20	33.05	6.83	7.37	3.30	1.40	9.07	3.24	44.66	50.50	60.50	92.33	0.89
MnO	%	0.002	0.013	0.007	0.012	0.008	0.007	0.009	0.006	0.008	0.010	18.479	0.006	0.007	0.132	0.008
MgO	%	0.01	0.10	0.06	0.10	0.11	0.34	1.29	0.71	0.78	0.74	0.33	0.07	0.04	0.08	0.06
CaO	%	0.001	0.09	0.06	0.09	0.05	0.19	0.38	0.26	0.36	0.33	0.11	0.06	0.02	0.02	0.22
Na2O	%	0.01	<0.01	0.05	0.04	0.04	0.07	0.23	0.17	0.11	0.11	0.15	<0.01	<0.01	<0.01	4.36
K2O	%	0.001	0.10	0.02	0.06	0.55	0.69	1.51	1.36	1.22	1.21	1.54	0.05	0.06	0.01	4.73
TiO2	%	0.003	0.98	1.28	1.23	0.63	0.57	0.67	1.03	0.94	0.89	0.25	1.04	0.70	1.05	0.19
P2O5	%	0.002	0.059	0.051	0.023	0.027	0.041	0.057	0.073	0.145	0.108	0.303	0.083	0.068	0.105	0.042
LOI	%		7.73	9.89	10.14	2.79	4.82	7.15	8.15	7.95	9.20	10.88	10.90	10.64	2.16	1.11
Ba	ppm	30	776	821	466	231	197	631	237	271	386	4981	105	21	168	604
Ce	ppm	20	<20	23	22	<20	32	31	54	83	72	69	35	<20	25	101
Cl	ppm	20	<20	40	80	<20	<20	210	200	30	<20	20	190	20	<20	210
Cr	ppm	10	413	367	438	31	65	42	39	42	45	<10	129	153	16	<10
Co	ppm	10	22	<10	<10	<10	<10	<10	<10	<10	<10	1678	12	18	136	<10
Cu	ppm	10	18	16	25	17	<10	37	<10	<10	11	309	115	258	<10	11
Ga	ppm	3	27	33	26	11	17	17	24	21	23	7	37	28	17	20
La	ppm	10	<10	<10	11	<10	22	26	32	49	34	16	<10	<10	<10	64
Ni	ppm	10	<10	<10	22	<10	<10	38	101	19	44	1569	<10	<10	77	21
Nb	ppm	4	5	14	11	6	6	4	5	<4	<4	<4	27	15	4	19
Pb	ppm	5	55	60	235	14	28	15	22	28	24	50	9	17	<5	16
Rb	ppm	5	5	<5	<5	27	31	61	67	58	68	62	<5	<5	<5	239
S	ppm	10	550	550	580	50	160	680	160	220	180	140	850	410	340	20
Sr	ppm	5	51	31	32	28	102	125	266	530	319	364	12	7	7	79
V	ppm	5	2552	2313	8914	215	427	128	103	169	157	81	705	603	263	8
Y	ppm	5	15	22	24	8	13	64	17	16	17	28	7	8	<5	59
Zn	ppm	5	39	60	60	<5	18	124	23	32	33	2145	28	28	127	20
Zr	ppm	5	257	313	289	119	138	118	175	159	148	54	300	214	<5	164

F	Feldspar	Li	Lithiophorite
Gt	Goethite	M	Mica
Hm	Hematite	Op	Opal CT
Ho	Hollandite	Q,	Quartz
K	Kaolinite	Sm	Smectite

Table A2 : Geochemistry of RAB drill hole ROTR 155 at Tringadee Prospect.

Sample No				TG1AB	TG4AB	TG6AB	TG8G	TG12G	TG15AB	TG15G	TG17AB	TG17G	TG21AB1	TG21AB2	TG21AB3	TG27AB	TG30AB	TG31G	TG32G	TG33G
Depth (m)				0.5	3.5	5.5	7.5	11.5	14.5	14.5	16.5	16.5	20.5	20.5	20.5	26.5	29.5	32.5	36.5	39.5
Size fraction (µm)				>710	>710	>710	<710	<710	>710	<710	>710	<710	>710	>710	>710	>710	>710	<710	<710	<710
Regolith Unit				Saprolite	Saprolite	Saprolite	Saprolite	Saprolite	Fe-band	Saprolite	Fe-band	Saprolite	Fe-band (Mn rich)	Fe-band (goethitic)	Fe-band (goethitic)	Saprolite	Fe-band	Saprolite	Saprolite	Black Shale
Element	Unit	Detection Limit	Method																	
SiO2	%	0.01	XRF	61.07	69.41	63.71	68.14	69.37	39.54	67.77	45.92	68.02	19.32	26.91	47.99	69.82	46.54	66.59	87.21	54.31
Al2O3	%	0.01	XRF	17.20	18.34	16.50	16.54	16.52	8.95	14.29	10.25	14.39	4.65	6.50	10.60	9.06	7.02	13.74	5.46	18.68
Fe2O3	%	0.01	XRF	8.58	1.47	7.89	3.57	2.38	38.98	5.50	33.41	3.86	18.25	50.75	26.59	9.60	30.45	4.40	2.02	6.54
MgO	%	0.01	XRF	0.50	0.30	0.24	0.59	0.81	0.31	0.78	0.32	1.22	0.38	0.54	1.04	0.88	0.33	1.39	0.21	0.78
CaO	%	0.001	XRF	0.25	0.08	0.46	0.28	0.19	0.20	0.27	0.10	0.30	0.17	0.13	0.26	0.22	0.12	0.37	0.06	0.20
Na2O	%	0.01	XRF	0.08	0.10	0.08	0.12	0.24	0.07	0.15	0.10	0.22	0.15	0.08	0.15	0.18	0.11	0.26	0.28	0.13
K2O	%	0.001	XRF	0.88	0.91	0.81	0.94	1.08	0.63	1.10	0.70	1.35	3.26	0.91	1.26	1.09	1.22	1.77	1.86	3.12
TiO2	%	0.001	XRF	0.75	0.75	0.68	0.71	0.75	0.42	0.67	0.44	0.71	0.21	0.33	0.46	0.41	0.26	0.69	0.52	0.95
P2O5	%	0.002	XRF	0.148	0.192	0.198	0.140	0.045	0.572	0.092	0.322	0.052	0.258	0.547	0.266	0.230	0.637	0.132	0.052	0.114
MnO	%	0.002	XRF	0.012	0.005	0.008	0.007	0.010	0.565	0.030	1.026	0.027	41.581	2.540	0.280	0.094	4.262	0.023	0.022	0.022
LOI	%		XRF	8.04	6.95	7.64	6.78	6.25	8.62	6.05	5.91	6.01	10.14	•	7.92	4.89	7.44	6.20	1.52	11.62
Cr	ppm	5	NAA	49.8	32.9	39.6	49.7	67.5	39.3	48	117	47	16.7	42.1	39	46.8	52	57.4	19.6	53.7
V	ppm	5	XRF	216	92	224	151	126	291	138	432	144	174	237	140	135	357	154	34	96
Cu	ppm	10	XRF	<10	<10	19	<10	<10	167	34	45	33	62	27	<10	16	59	13	<10	<10
Pb	ppm	5	XRF	23	26	18	29	13	91	16	64	16	204	19	17	23	86	20	16	24
Zn	ppm	5	XRF	20	10	22	32	58	1659	242	557	203	1359	1601	991	244	522	93	18	35
Ni	ppm	10	XRF	<10	<10	<10	<10	10	500	61	185	39	880	512	393	64	326	35	10	15
Co	ppm	1	NAA	1.81	<1	1.18	1.38	2.98	233	21.7	171	11.6	2080	386	177	20.3	440	9.03	1.99	4.45
As	ppm	1	NAA	11.1	<1	12.3	4.63	1.35	20.2	4.24	26	2.89	10.5	32.1	13.2	16.1	51.2	5.05	1.26	7.13
Sb	ppm	0.2	NAA	0.28	<0.2	0.22	<0.2	0.25	0.42	0.41	0.76	0.25	<0.2	0.63	0.43	0.54	0.77	<0.2	<0.2	<0.2
Mo	ppm	5	NAA	<5	<5	<5	<5	<5	<5	<5	<5	<5	<5	<5	<5	<5	<5	<5	<5	<5
Ag	ppm	5	NAA	<5	<5	<5	<5	<5	<5	<5	<5	<5	<10	<5	<5	<5	<5	<5	<5	<5
Ga	ppm	3	XRF	18	18	19	19	20	15	16	13	18	<3	8	18	14	11	15	6	22
W	ppm	2	NAA	<2	<2	<2	<2	<2	<2	<2	<2	<2	<2	<2	<2	<2	<2	<2	3.47	2.95
Ba	ppm	30	XRF	217	643	272	294	197	746	206	2196	204	15608	951	240	244	9690	218	248	404
Zr	ppm	5	XRF	146	139	130	132	131	91	127	107	133	47	69	92	72	69	122	147	412
Nb	ppm	4	XRF	8	5	4	7	7	10	8	<2	6	<4	5	<4	4	<4	6	11	27
Au	ppb	5	NAA	<5	<5	<5	<5	<5	<5	<5	<5	<5	<5	<5	<5	<5	<5	<5	<5	<5
Ce	ppm	2	NAA	44.7	139	67.6	88.7	42.1	57.6	46.5	52.6	40.8	147	28.8	30.2	21.5	95.3	50.7	71.5	140
Cs	ppm	1	NAA	3.12	3.32	3.17	2.75	3.88	6.36	7.65	3.59	11.1	8.36	12.6	15.3	4.26	2.67	3.9	2.27	6.31
Eu	ppm	0.5	NAA	<0.5	4.1	1.48	2.98	2.31	7.39	3.77	2.06	1.82	1.29	1.06	0.89	<0.5	2.36	0.98	0.82	1.72
Hf	ppm	0.5	NAA	4.01	4.16	3.44	3.4	3.53	2.34	3.43	2.45	3.51	<0.5	1.58	2.43	2.08	1.69	3.23	4.24	11.3
Ir	ppb	20	NAA	<20	<20	<20	<20	<20	<20	<20	<20	<20	<20	<20	<20	<20	<20	<20	<20	<20
La	ppm	0.5	NAA	24.4	54.3	27.5	33.3	20	20.6	20.4	20.1	20.4	26.6	11.5	15.2	11.7	28.4	22.6	36.7	73.3
Lu	ppm	0.2	NAA	0.22	0.23	0.34	0.81	0.42	3.37	1.18	0.54	0.47	0.28	0.33	0.26	<0.2	0.26	0.26	0.37	0.74
Rb	ppm	5	XRF	37	38	38	45	51	37	65	29	84	75	61	77	53	44	72	68	154
Sm	ppm	0.2	NAA	2.63	18.6	6.97	10.1	7.45	16.2	9.77	7.21	5.71	5.16	3.68	3.49	2.29	10.1	4.98	5.02	9.76
Sc	ppm	0.1	NAA	16.8	11.4	13.1	15.5	13.3	18.4	12.2	13.1	12.4	5.05	12.1	12.2	10.7	12.2	13.2	4.25	13
Se	ppm	5	NAA	<5	<5	<5	<5	<5	<5	<5	<5	<5	<5	<5	<5	<5	<5	<5	<5	<5
Ta	ppm	1	NAA	<1	<1	<1	<1	<1	1.11	1.52	<1	<1	<1	<1	<1	<1	<1	1.1	1.23	3.48
Th	ppm	0.5	NAA	8.49	6.92	9.21	7.05	8.25	5.45	7.53	11.9	8.17	3.18	6.48	6.33	5.88	7.62	7.55	12.8	23.6
Yb	ppm	0.5	NAA	1.64	1.5	2.61	5.87	3.2	24.2	8.74	3.72	3.47	2.05	2.3	2.14	1.72	2.19	1.87	2.6	5.33
Br	ppm	2	NAA	2.22	3.28	<2	<2	<2	<2	2.87	2.36	6.35	<2	2.51	5.18	<2	<2	<2	<2	2.2
Sr	ppm	5	XRF	158	573	256	333	76	241	72	157	61	255	50	51	45	298	61	25	33
U	ppm	2	NAA	<2	<2	<2	<2	<2	4.98	2.48	<2	<2	<2	2.09	<2	<2	<2	<2	<2	5.32
Y	ppm	5	XRF	15	13	22	66	32	300	104	30	32	22	25	22	17	19	18	26	48
Cl	ppm	20	XRF	<20	<20	<20	<20	350	<20	<20	<20	<20	<20	<20	<20	<20	<20	<20	<20	<20
S	ppm	10	XRF	1380	780	1920	460	340	900	240	790	210	150	180	220	180	2260	460	1080	11600

Table A3 : Geochemistry of RAB drill hole ROTR 156 at Tringadee Prospect.

Sample No				TG34AB	TG37AB	TG39AB	TG41AB	TG45G	TG50AB	TG53AB	TG57AB1	TG57AB2	TG57AB3	TG60AB	TG62AB	TG65G	TG66G
Depth(m)				0.5	3.5	5.5	7.5	11.5	16.5	19.5	23.5	23.5	23.5	26.5	28.5	35.5	38.5
Size fraction (µm)				>710	>710	>710	>710	<710	>710	>710	>710	>710	>710	>710	>710	<710	<710
Regolith Unit				Saprolite	Saprolite	Saprolite	Fe-band	Saprolite	Saprolite	Saprolite	Fe-band (Mn rich)	Fe-band (goethitic)	Fe-band (goethitic)	Fe-band	Saprolite	Saprolite	Black shale
Element	Unit	Detection Limit	Method														
SiO2	%	0.01	XRF	63.81	65.08	52.17	24.81	70.74	53.40	54.37	13.85	32.65	52.74	35.52	51.95	83.66	49.12
Al2O3	%	0.01	XRF	14.56	20.31	15.24	7.08	14.60	14.40	15.15	3.42	6.43	10.27	9.03	12.79	6.73	19.49
Fe2O3	%	0.01	XRF	9.47	1.83	19.87	55.52	3.30	19.28	17.13	3.25	49.17	24.72	37.20	22.55	3.12	7.50
MgO	%	0.01	XRF	0.45	0.31	0.34	0.17	0.81	0.44	0.46	0.21	0.54	0.82	0.60	0.44	0.31	0.70
CaO	%	0.001	XRF	0.27	0.42	0.23	0.22	0.27	0.14	0.17	0.16	0.10	0.19	0.21	0.15	0.07	0.46
Na2O	%	0.01	XRF	0.09	0.07	0.08	0.03	0.13	0.11	0.11	0.14	0.09	0.10	0.11	0.10	0.23	0.17
K2O	%	0.001	XRF	0.81	0.93	0.81	0.39	1.06	0.73	0.86	4.07	0.87	1.20	1.03	0.82	1.92	2.62
TiO2	%	0.001	XRF	0.71	0.81	0.69	0.38	0.65	0.64	0.64	0.16	0.33	0.46	0.39	0.53	0.47	0.91
P2O5	%	0.002	XRF	0.156	0.109	0.327	0.863	0.076	0.323	0.386	0.153	0.419	0.244	0.553	0.429	0.084	0.105
MnO	%	0.002	XRF	0.014	0.005	0.012	0.014	0.017	0.036	0.026	60.773	0.139	0.041	4.648	0.646	0.019	0.016
LOI	%		XRF	7.10	7.84	8.33	10.23	5.98	8.28	8.59	•	8.85	7.28	9.27	7.99	2.30	15.01
Cr	ppm	5	NAA	48.7	41.9	49.8	69.9	43.5	79.1	47.7	<5	27.4	40.9	41.1	67.1	23.3	54
V	ppm	5	XRF	221	127	339	381	138	310	230	287	112	134	236	320	44	109
Cu	ppm	10	XRF	3	<10	<10	25	18	27	25	98	<10	<10	57	7	<10	12
Pb	ppm	5	XRF	18	19	39	7	19	27	50	209	14	32	120	65	15	26
Zn	ppm	5	XRF	21	12	50	347	95	216	272	1401	1161	662	869	225	19	37
Ni	ppm	10	XRF	<10	<10	10	111	18	63	81	1064	274	201	498	145	<10	16
Co	ppm	1	NAA	2.41	<1	2.14	17.1	5.34	20.6	23.8	2620	90.9	49.7	367	158	2.46	4.39
As	ppm	1	NAA	14.7	2.9	28	44.4	3.3	22.5	17.7	6.09	17.4	12.4	27	29.9	2.87	8.15
Sb	ppm	0.2	NAA	0.3	0.26	<0.2	0.46	0.22	0.34	<0.2	0.99	0.41	0.33	0.37	0.49	<0.2	<0.2
Mo	ppm	5	NAA	<5	<5	<5	<5	<5	<5	<5	<5	<5	<5	<5	<5	<5	<5
Ag	ppm	5	NAA	<5	<5	<5	<5	<5	<5	<5	<5	<5	<5	<5	<5	<5	<5
Ga	ppm	3	XRF	19	21	20	12	15	21	16	4	7	12	15	19	9	24
W	ppm	2	NAA	<2	<2	<2	<2	<2	<2	<2	<4	<2	<2	<2	<2	4.01	3.02
Ba	ppm	30	XRF	224	294	315	52	204	278	370	32582	196	270	2741	689	264	293
Zr	ppm	5	XRF	138	145	134	74	112	131	139	45	73	95	84	107	135	305
Nb	ppm	4	XRF	6	9	7	7	6	6	5	<5	3	6	0	2	7	25
Au	ppb	5	NAA	<5	<5	<5	<5	<5	<5	<5	<5	<5	<5	<5	<5	<5	<5
Ce	ppm	2	NAA	60.3	103	97.1	19.5	63.1	77.2	168	251	26.4	43.1	84	110	60.4	111
Cs	ppm	1	NAA	2.55	2.83	2.34	2.59	6.69	3.52	3.42	3.81	8.29	7.34	4.04	2.58	2.64	5.36
Eu	ppm	0.5	NAA	0.84	2.43	1.48	1.02	9.68	1.08	2.34	2.31	1.14	1.26	1.43	1.55	0.77	1.31
Hf	ppm	0.5	NAA	3.39	3.94	3.71	1.36	3.26	3.35	3.02	0.94	1.86	3.04	2.3	2.51	3.96	8.84
Ir	ppb	20	NAA	<20	<20	<20	<20	<20	<20	<20	<20	<20	<20	<20	<20	<20	<20
La	ppm	0.5	NAA	29.3	42.8	40.3	10	23.7	35	73	46.8	11.6	20.7	19.7	47.4	31.3	60.5
Lu	ppm	0.2	NAA	0.25	0.91	0.2	0.31	1.82	0.3	0.33	0.27	0.46	0.32	0.35	0.28	0.34	0.56
Rb	ppm	5	XRF	32	43	35	22	57	34	36	58	67	72	50	30	72	137
Sm	ppm	0.2	NAA	3.96	8.74	7.53	3.11	26.4	5.53	12	8.46	3.96	4.91	5.29	8.04	4.25	7.94
Sc	ppm	0.1	NAA	13.3	10.7	19.8	39.1	12.2	20.4	28.3	4.47	9.32	11	12.7	20.1	5.55	12.6
Se	ppm	5	NAA	<5	<5	<5	<5	<5	<5	<5	<5	<5	<5	<5	<5	<5	<5
Ta	ppm	1	NAA	<1	<1	1.42	<1	1.32	<1	<1	3.02	<1	<1	<1	<1	1.44	1.69
Th	ppm	0.5	NAA	9.1	8.23	11	8.14	7.35	9.81	10.1	3.3	4.17	5.96	6.13	9.75	11.5	21.5
Yb	ppm	0.5	NAA	1.88	7.06	1.81	2.61	13.4	2.38	2.49	2.46	3.18	2.47	3.07	2.22	2.35	3.95
Br	ppm	2	NAA	2.36	3.13	3.92	2.24	<2	2.75	2.42	2.91	<2	<2	<2	2.3	<2	<2
Sr	ppm	5	XRF	180	308	347	55	77	244	592	210	27	61	109	354	28	34
U	ppm	2	NAA	<2	<2	<2	<2	<2	2.41	<2	<2	<2	<2	<2	<2	<2	4.63
Y	ppm	5	XRF	18	60	12	15	155	18	19	24	29	21	32	17	24	40
Cl	ppm	20	XRF	<20	<20	<20	<20	<20	<20	<20	<20	<20	<20	<20	20	<20	<20
S	ppm	10	XRF	370	1490	1240	2210	410	930	1960	150	150	240	570	2090	980	13260

Table A4 : Geochemistry of ferruginous veins at Brumby Prospect.

Sample No				TG-215	TG-109	TG-108	TG-214	TG-213	TG-112	TG-113	TG-212	TG-210	TG-209	TG-208
Northing (m)				7584400	7584400	7584400	7584400	7584400	7584400	7584400	7584400	7584400	7584400	7584400
Easting (m)				475000	475050	475070	475080	475100	475150	475155	475250	475460	475480	475500
Element	Unit	Detection Limit	Method											
SiO2	%	0.01	XRF	47.3	36.84	39.08	38.25	30.92	31.16	44.43	36.11	32.94	44.58	46.32
Al2O3	%	0.01	XRF	9.09	9.79	8.2	10.15	4.88	6.47	3.87	6.91	8.29	9.53	9.35
Fe2O3	%	0.005	XRF	35.08	43.33	46.67	41.52	57.41	54.96	46.53	48.85	48.00	37.04	34.53
MgO	%	0.01	XRF	0.13	0.09	0.09	0.11	0.07	0.08	0.07	0.12	0.09	0.12	0.11
CaO	%	0.00	XRF	0.06	0.11	0.04	0.03	0.03	0.01	0.00	0.23	0.02	0.05	0.02
Na2O	%	0.01	XRF	0.04	0.04	0.04	0.03	0.04	0.03	0.04	0.07	0.04	0.03	0.05
K2O	%	0.001	XRF	0.36	0.3	0.33	0.33	0.3	0.27	0.32	0.39	0.37	0.36	0.35
TiO2	%	0.003	XRF	0.34	0.36	0.36	0.36	0.33	0.31	0.12	0.39	0.4	0.37	0.36
P2O5	%	0.002	XRF	0.472	0.477	0.111	0.49	0.396	0.305	0.299	0.302	0.955	0.314	0.351
MnO	%	0.002	XRF	0.011	0.02	0.109	0.021	0.059	0.009	0.069	0.031	0.012	0.017	0.018
LOI	%		XRF	7.43	8.86	5.46	9.06	5.52	6.56	4.58	6.48	8.9	7.53	7.63
Cr	ppm	5	NAA	95.5	283	72.3	160	124	150	22.1	91.1	264	215	128
V	ppm	5	XRF	440	1374	778	1305	1072	349	62	537	554	1491	1046
Cu	ppm	10	XRF	22	11	<10	17	<10	13	<10	<10	36	14	31
Pb	ppm	5	XRF	18	6	<5	27	<5	<5	<5	10	<5	26	21
Zn	ppm	5	XRF	37	35	20	32	49	65	1423	37	54	24	26
Ni	ppm	10	XRF	6	<10	<10	3	<10	<10	216	<10	<10	<10	<10
Co	ppm	1	NAA	1.77	1.37	<1	<1	2.34	3.3	112	1.3	1.05	1.57	<1
As	ppm	1	NAA	24.8	74.9	16.6	52.3	55.2	15.6	7.95	33.5	40.1	44.2	38.6
Sb	ppm	0.2	NAA	<0.2	<0.2	<0.2	<0.2	<0.2	<0.2	<0.2	1.9	<0.2	0.34	<0.2
Mo	ppm	5	NAA	<5	<5	<5	<5	<5	<5	<5	<5	<5	<5	<5
Ag	ppm	5	NAA	<5	<5	<5	<5	<5	<5	<5	<5	<5	<5	<5
Ga	ppm	3	XRF	15	25	13	26	16	13	<3	10	23	26	27
W	ppm	2	NAA	<2	<2	<2	<2	<2	<2	<2	<2	<2	<2	0.67
Ba	ppm	30	XRF	232	156	390	123	540	203	18	464	294	323	108
Zr	ppm	5	XRF	78	70	65	75	57	67	50	96	74	80	71
Nb	ppm	4	XRF	<4	4	<4	<4	7	<4	<4	<4	4	<4	<4
Au	ppb	5	NAA	<5	<5	<5	<5	<5	<5	<5	<5	<5	<5	<5
Ce	ppm	2	NAA	37.9	29.8	22.4	27.9	50.9	35	12.6	77.3	45.4	44.1	20.5
Cs	ppm	1	NAA	<1	<1	1.96	1.14	2	1.11	<1	1.6	3.38	<1	<1
Eu	ppm	0.5	NAA	0.67	0.58	0.53	0.5	1.43	0.7	0.88	1.11	2.27	0.7	<0.5
Hf	ppm	0.5	NAA	2	1.89	1.89	1.9	1.65	2.02	1.3	2.1	1.62	2.25	1.48
Ir	ppb	20	NAA	<20	<20	<20	<20	<20	<20	<20	<20	<20	<20	<20
La	ppm	0.5	NAA	17.2	13.1	11.2	15.8	20	16.6	4.12	32.6	17.7	22.9	12.1
Lu	ppm	0.2	NAA	<0.2	<0.2	<0.2	<0.2	<0.2	<0.2	<0.2	<0.2	<0.2	<0.2	<0.2
Rb	ppm	5	XRF	12	13	18	4	17	7	18	18	17	11	10
Sm	ppm	0.2	NAA	4.19	3.64	2.8	2.31	7.89	3.78	2.52	6.15	10.9	4.18	1.56
Sc	ppm	0.1	NAA	20.5	27.2	15.3	25.6	30.5	23	29.2	24.3	29.6	18.1	22
Se	ppm	5	NAA	<5	<5	<5	<5	<5	<5	<5	<5	<5	8	7
Ta	ppm	1	NAA	<1	<1	<1	<1	<1	<1	<1	<1	<1	<1	<1
Th	ppm	0.5	NAA	9.82	26.1	11.2	25.4	12.8	11.5	2.34	9.22	14.6	22.4	30.4
Yb	ppm	0.5	NAA	1.06	0.82	0.81	0.61	1.4	1.01	2.83	1.31	1.08	0.82	0.58
Br	ppm	2	NAA	<2	2.13	4.19	<2	<2	<2	<2	7.03	<2	3.03	2.02
Sr	ppm	5	XRF	96	96	67	67	105	84	17	286	81	92	43
U	ppm	2	NAA	3.66	<2	<2	<2	2.65	<2	4.88	<2	<2	<2	<2
Y	ppm	5	XRF	7	5	5	8	10	7	37	7	6	7	12
Cl	ppm	20	XRF	150	140	<20	50	60	190	<20	1070	<20	<20	<20
S	ppm	10	XRF	950	1320	1160	1290	1260	1660	780	2340	910	790	960

Table A5 : Geochemistry of percussion drill hole PETD 6 at Brumby prospect.

Depth (m)				1	2	6	8	9	12	15	17	20	24	25	28	30	34	37	39	43	48	52	55
Element	Unit	Detection Limit	Method																				
SiO2	%	0.01	XRF	74.48	65.81	69.94	69.11	60.61	91.9	95.5	93.77	96.32	68.28	31.84	69.82	70.82	41.79	34.47	33.92	28.26	64.66	53.21	41.33
Al2O3	%	0.01	XRF	14.46	12.35	18	14.97	12.35	3.47	1.95	2.45	0.99	2.22	3.08	10.55	17.92	10.51	11.03	18.11	9.58	15.17	10.15	10.61
Fe2O3	%	0.01	XRF	2.51	13.21	2.13	6.76	16.9	2.87	1.83	2.22	2.5	24.62	57.96	13.33	2.63	39.25	44.6	30.3	50.09	7.05	26.21	33.54
MgO	%	0.01	XRF	0.16	0.13	0.15	0.16	0.15	0.06	0.04	0.05	0.02	0.07	0.08	0.07	0.13	0.2	0.35	0.85	0.8	0.72	0.35	0.93
CaO	%	0.001	XRF	0.07	0.04	0.07	0.04	0.04	0.02	0.02	0.01	0.02	0.05	0.04	0.06	0.11	0.17	0.21	0.42	0.26	0.51	0.92	2.1
Na2O	%	0.01	XRF	0.1	0.07	0.09	0.1	0.09	0.03	0.01	0.02	0.01	0.03	0.04	0.03	0.06	0.02	0.04	0.08	0.11	4.69	4.35	4.27
K2O	%	0.001	XRF	0.64	0.53	0.64	0.7	0.65	0.49	0.35	0.55	0.23	0.29	0.33	0.25	0.38	0.11	0.23	0.64	0.6	3.41	0.77	1.18
TiO2	%	0.001	XRF	0.59	0.52	0.67	0.67	0.63	0.3	0.2	0.19	0.05	0.21	0.68	0.22	0.06	0.24	0.44	1.59	0.36	0.41	0.31	0.41
P2O5	%	0.002	XRF	0.07	0.263	0.169	0.136	0.261	0.041	0.029	0.034	0.034	0.342	0.423	0.08	0.019	0.31	0.33	0.192	0.188	0.08	0.269	0.309
MnO	%	0.002	XRF	0.009	0.015	0.006	0.009	0.011	0.013	0.011	0.011	0.011	0.048	0.044	0.091	0.018	0.33	0.164	0.083	0.053	0.032	0.031	0.042
LOI	%		XRF	6.35	6.84	7.11	6.71	7.18	1.09	0.49	0.64	0.28	3.63	5.95	5.07	6.75	6.21	7.13	11.01	8.18	2.04	1.83	3.8
Cr	ppm	5	NAA	49.6	62.6	37.2	46.5	52.2	18.1	13.3	12.6	10.8	23.2	44.4	29.1	9.1	16.4	28.8	103	24.4	43.7	33	24.5
V	ppm	5	XRF	73	294	93	150	228	22	9	16	10	70	217	99	26	231	277	328	213	57	129	190
Cu	ppm	10	XRF	<10	33	<10	12	44	<10	<10	<10	<10	84	245	537	362	1699	1866	1952	3772	1034	8271	7913
Pb	ppm	5	XRF	18	15	21	19	10	10	7	10	11	19	<5	23	6	17	5	16	10	17	20	6
Zn	ppm	5	XRF	22	35	14	18	47	86	20	18	17	93	184	45	26	84	90	132	80	42	36	43
Ni	ppm	10	XRF	<10	<10	<10	<10	<10	<10	<10	<10	<10	30	44	33	27	53	58	77	53	26	42	26
Co	ppm	1	NAA	<1	<1	<1	1.37	1.91	3.35	1.76	1.35	1.67	16.1	19.7	19.8	4.21	182	112	96.5	111	53.7	186	176
As	ppm	1	NAA	2.02	11.9	3.18	6.51	10.2	1.13	<1	<1	1.09	3.02	4.7	4.02	1.32	<1	<1	<1	<1	<1	1.59	2.79
Sb	ppm	0.2	NAA	0.26	0.06	0.83	0.85	0.3	0.06	0.06	0.26	0.2	0.21	<0.2	0.33	0.31	<0.2	<0.2	<0.2	0.45	<0.2	0.39	<0.2
Mo	ppm	5	NAA	<5	<5	<5	<5	<5	<5	<5	<5	<5	<5	<5	<5	<5	<5	<5	<5	<5	<5	<5	<5
Ag	ppm	5	NAA	<5	<5	<5	<5	<5	<5	<5	<5	<5	<5	<5	<5	<5	<5	<5	<5	<5	<5	<5	<5
Ga	ppm	3	XRF	15	17	17	17	19	4	3	3	<3	3	17	16	18	20	22	30	24	18	15	20
W	ppm	2	NAA	<2	<2	<2	<2	<2	11.4	8.25	6.68	2.61	3.86	16.6	<2	<2	<2	<2	<2	<2	<2	<2	<2
Ba	ppm	30	XRF	310	277	446	212	177	479	150	153	36	95	69	123	<30	451	425	270	572	445	199	737
Zr	ppm	5	XRF	129	111	130	125	124	115	82	82	52	47	80	35	12	90	134	131	113	142	191	101
Nb	ppm	4	XRF	<4	<4	<4	<4	<4	<4	<4	<4	<4	<4	<4	<4	<4	<4	<4	<4	<4	7	<4	<4
Au	ppb	5	NAA	<5	<5	7.6	<5	<5	<5	<5	<5	<5	<5	20.8	15.5	8.8	14.5	79.4	338	76	<5	75.2	54.9
Ce	ppm	2	NAA	82	68.5	81.3	45.3	39.8	37.3	22.4	20.6	12.3	19.8	29	13.5	9.63	341	483	365	313	71.8	57.3	88.7
Cs	ppm	1	NAA	2.42	3.09	2.76	4.2	3.77	<1	<1	<1	<1	1.2	1.87	<1	<1	1.99	4.47	4.6	7.16	2.02	<1	<1
Eu	ppm	0.5	NAA	1.39	1.83	8.99	1.76	1.19	0.58	<0.5	<0.5	<0.5	0.89	0.96	<0.5	<0.5	2.81	5.52	7.9	7.61	0.77	0.8	1.36
Hf	ppm	0.5	NAA	3.48	3.02	3.97	3.37	3.41	3.55	2.41	2.55	1.33	1.56	1.94	1.33	0.5	2.19	3.61	4.4	3.59	4.03	4.93	2.31
Ir	ppb	20	NAA	<20	<20	<20	<20	<20	<20	<20	<20	<20	<20	<20	<20	<20	<20	<20	<20	<20	<20	<20	<20
La	ppm	0.5	NAA	32	26.4	38.7	22	18.9	19.6	10.6	10	6.36	8.09	21.3	18.8	10.7	126	166	158	204	36.5	25.4	47.1
Lu	ppm	0.2	NAA	0.2	<0.2	0.3	0.29	0.28	0.34	<0.2	<0.2	<0.2	0.26	0.33	0.21	<0.2	1.28	2.52	8.21	2.79	0.4	0.56	0.59
Rb	ppm	5	XRF	30	26	34	35	33	21	12	18	6	7	23	17	26	20	45	84	84	154	29	33
Sm	ppm	0.2	NAA	7.81	10.4	43.8	7.87	5.09	4	2.09	1.81	1.2	3.33	3.11	1.61	1.07	18.5	29.8	44.6	46.9	5.71	4.55	6.49
Sc	ppm	0.1	NAA	8.38	23.8	10.3	12.7	18	5.03	2.65	2.93	1.49	6.47	10.1	9.74	2.74	8.52	7.59	31.7	5.87	7.54	5.38	9.86
Se	ppm	5	NAA	<5	<5	<5	<5	<5	<5	<5	<5	<5	<5	<5	<5	<5	<5	<5	<5	<5	<5	19.6	<5
Ta	ppm	1	NAA	<1	1.05	1.29	1.2	1.31	1.11	1.14	<1	<1	<1	<1	<1	<1	<1	<1	3.45	<1	1.76	2.62	<1
Th	ppm	0.5	NAA	6.27	12.5	9.44	7.75	8.93	6.59	3.7	3.58	2.29	8.66	17.1	8.39	1.61	70.7	67.9	26.1	29.2	14	14	8.48
Yb	ppm	0.5	NAA	1.64	1.62	2.07	2.08	2.37	2.53	1.41	1.32	0.77	2.02	2.99	1.52	1.08	8.4	16.6	51.2	17.6	2.72	3.43	4.04
Br	ppm	2	NAA	2.88	<2	<2	<2	<2	<2	<2	<2	<2	<2	<2	<2	<2	<2	<2	<2	<2	<2	<2	2.18
Sr	ppm	5	XRF	120	124	231	124	94	26	21	15	12	121	46	17	14	74	82	39	78	71	69	66
U	ppm	2	NAA	<2	2.95	0.67	2.1	<2	<2	<2	<2	<2	11.2	16.1	13	3.32	11.9	12.9	24.5	7.59	5.69	5.11	2.26
Y	ppm	5	XRF	13	15	18	16	16	24	12	12	8	15	16	9	13	133	144	393	120	22	24	27
Cl	ppm	20	XRF	330	70	70	100	80	20	50	20	80	60	20	250	100	130	130	210	70	520	170	140
S	ppm	10	XRF	220	650	340	370	640	220	100	80	100	1090	930	230	140	190	160	260	150	100	990	14450

TRINGADEE AREA Regolith - Landforms

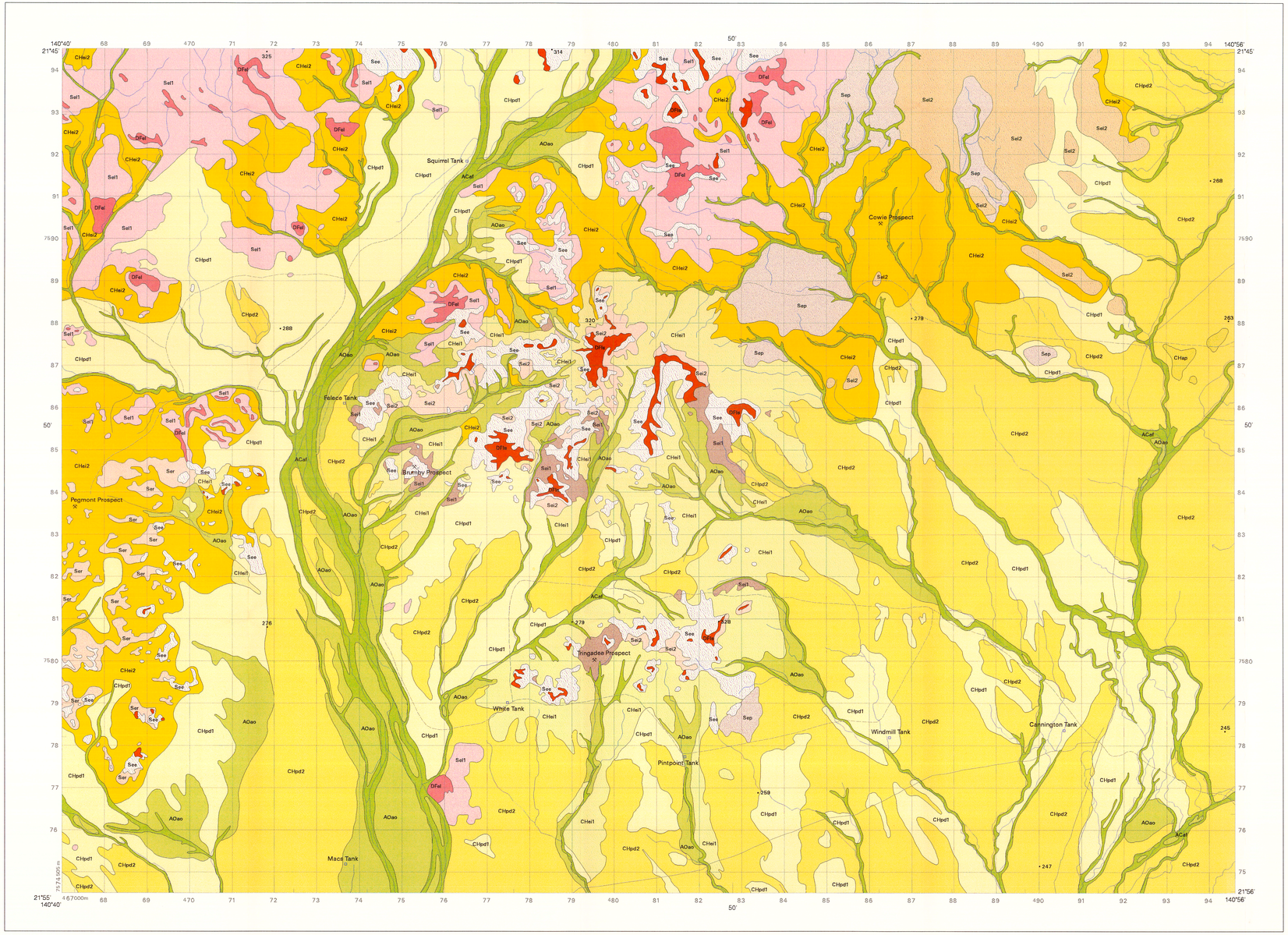

REGOLITH TYPES

Major bedrock type

Duricrust

Proterozoic bedrock

Ferruginous

Granite — **DFel** — *Lag of lateritic nodules and mottles. Patchy mottled ferruginous duricrust, in places silicified, which overlies mottled /ferruginous saprolite and pale saprolite. Silicification of the saprolite is common. Low hills (30 - 90m relief).*

Post Proterozoic

Ferruginous

Mesozoic sediments — **DFls** — *Lag of lateritic nodules, mottles and mottled saprolite fragments. Patchy silicified mottled duricrust overlies brecciated silicified mottled saprolite and silicified saprolite. Mesa, plateaux and buttes.*

Saprolite

Proterozoic bedrock

Proterozoic bedrock

- **Sel1** — *Lag of saprolite fragments, in places ferruginous. Mottled or pale silicified saprolite, occasional outcropping of weathered granite. Low hills (30 - 90m relief).*
- **Sep** — *Lag of lithic fragments on red sand. Ferruginous bedrock develops in dominantly gneiss and schist with minor amphibolite. Erosional plain (<9m relief)*
- **Ser** — *Lithosols and lithic fragments. Mottled saprolite, ferruginous saprolite develop in dominantly schistose metagreywacke/mica schist. Rises (9 - 30m relief).*
- **Sel2** — *Lithosols, lithic fragments develop in calc-silicate breccia and granofels, in places ferruginous. Low hills (30 - 90m relief).*

Post-Proterozoic bedrock

Mesozoic sediments

- **See** — *Collapsed and brecciated iron-stained silicified mottled saprolite, in places showing megamottling, overlying silicified pale saprolite. Escarpment.*
- **Sel1** — *Lag of goethite rich lithic fragments. Silicified pale saprolite with exposed goethitic rich subhorizontal veins which at times appear as small mounds. Pediments.*
- **Sei2** — *Silicified pale greyish saprolite with smectitic clays, highly erodible with deeply incised gullies. Pediments.*

Alluvial/colluvial sediments

- **ACaf** — *Recent alluvium of sands, gravels and sandy clay in confined channels. Floodplain.*
- **AOao** — *Recent alluvium of sands, gravels and sandy clay in poorly defined channels, overbank and channel overflow deposits. Floodout, overbank plain.*
- **CHei1** — *Polymictic lag of Fe-rich gravels and collapsed brecciated saprolite fragments (mainly derived from Mesozoic sediments) quartz gravels. Pediments.*
- **CHei2** — *Sheetflow deposits consisting of red sands, clay, quartz pebbles and minor ferruginous lag. Occassional subcropping of mottled saprolite developed dominantly from Proterozoic bedrock. Pediments.*
- **CHpd1** — *Reddish brown sheet flow deposits with polymictic ferruginous gravels, granules and quartz clasts. Depositional plain.*
- **CHpd2** — *Dark brown to black smectitic soils, 1-2m thick, with quartz gravels and gilgai microrelief. Depositional plain.*
- **CHap** — *Calcareous soils with fragments of limestone and quartz gravels. Alluvial plain.*

- *Minor Road*
- *Vehicle track*
- *River or creek*
- *Water Tank*
- *Spot height in metres*
- *Prospect*

REGOLITH CODES

DF	*Ferruginous duricrust*
S	*Saprolite*
AC	*Channel deposits*
AO	*Overbank deposits*
CH	*Sheet flow sediments*

LANDFORM CODES

ls	*Plateau*
el	*Pediments*
ep	*Erosional plain (<9m relief)*
es	*Escarpment*
or	*Rises (9-30m relief)*
ol	*Low hills (30-90m relief)*
af	*Floodplain*
ao	*Floodout, overbank plain*
pd	*Depositional plain*
ap	*Alluvial plain*

N

SCALE 1:50000

0.5 0 1 2 3 4 5 Kilometres

UNIVERSAL TRANSVERSE MERCATOR PROJECTION
LATITUDE OF ORIGIN: 0°. LONGITUDE OF ORIGIN: 129°

INDEX TO 1:100 000 MAPS
1:250 000 maps shown in blue

DUCHESS	MALBON 6855	MOUNT MEGILL 7055	McKINLAY 7155	EUDUNDA 7255	HAMILTON DOWNS 7355
DUCHESS			**McKINLAY**		
SF54-06			SF54-07		
CALVERTS 6854	MOUNT MEGILL 6954	ELVIRA 6954	EL BOSS 7154	KENILWORTH 7254	EADWORTH 7354
BUCKINGHAM 6853	DERBY DOWNS 6953	TOOLEBUC 7053	TWYNDYAM 7153	MIDDLETON 7253	JOHN HILLS 7353
BOULIA			**MACKUNDA**		
SF54-10			SF54-11		
BOULIA 6852	GOLDWOOD 6952	LUCKNOW 7052	MACKUNDA 7152	HILLS RANGE 7252	TULMUR 7352

MAP LOCALITY

Compiled by C.Phang (CRC LEME) and T.J.Munday (CRC AMET), 1997

Cartography by A.I.Johnston (AGSO), 1997
Geographic Information Systems by A.I.Johnston (AGSO), 1997

It is recommended that this map be referred to as:
C.Phang and T.J.Munday 1997 - Tringadee Area Regolith - Landforms (1:50,000 map scale). Cooperative Research Centre for Landscape Evolution and Mineral Exploration, (CRC LEME) Perth

Regolith-Landforms polygons are based on interpretation of 1:25,000 colour airphotos, Landsat TM image interpretation, field observations, and logging of RAB cuttings.

Published by CRC LEME, Perth, Australia.

Polygons shown on this map are derived from the AGSO Mt Isa 1:100,000 digital dataset and are © Copyright to the Commonwealth of Australia, AGSO.

Topographic information shown on this map has been derived from digital data supplied by the Australian Surveying and Land Information Group, Department of Administrative Services, Canberra, Australia
Base map © Crown Copyright, AUSLIG, Canberra, 1996

CRC LEME acknowledges the support provided for the production of this map by AMIRA.

AMIRA
Australian Mineral Industries Research Association Limited ACN 004 448 266

CRCLEME
Cooperative Research Centre for Landscape Evolution & Mineral Exploration

CRC LEME is an unincorporated joint venture between the Australian National University, University of Canberra, Australian Geological Survey Organisation and CSIRO Exploration and Mining, established and supported under the Australian Government's Cooperative Research Centres' Programme.

Appendix 1
C.Phang, T.J.Munday and J.E.Wildman, 1997. CRC LEME Restricted Report 58R/E&M Report 428R